科技部補助專題研究計畫成果報告
期末報告

雷射金屬沉積作業人員奈米暴露評估控制指標之開發與應用

計 畫 主 持 人： 王櫻芳
共 同 主 持 人： 闞斌如
計 畫 參 與 人 員： 碩士班研究生-兼任助理：席珮瑄
　　　　　　　　　碩士班研究生-兼任助理：蘇世心

報 告 附 件： 出席國際學術會議心得報告

中 華 民 國 107 年 09 月 20 日

中 文 摘 要 ：雷射金屬沉積作業(Laser Metal Deposition, LMD)列印技術已被廣泛應用於金屬模具、航太、鋼鐵、石化、機械五金等產業，該技術利用雷射能量讓同時間噴射出的金屬粉末材料熔融後覆蓋在母材上，並於母材上形成金屬保護層(抗腐蝕、抗磨耗、抗鏽蝕等)，或將金屬粉末熔融燒結後直接成型特殊造型體，而達到3D列印成型結構外形目的。雷射金屬沉積作業過程中，金屬粉末通過噴嘴自動施加，其所使用之雷射功率高達2000瓦之雷射源(溫度約1500℃或更高)，透過雷射產生熔池，進行沉積作業。然而，其所使用之材料金屬粉末會因受熱超過熔點而揮發逸散到空氣中隨之因環境溫度而使金屬蒸氣膠結而形成氧化金屬微粒，呼吸暴露於金屬燻煙可能引起潛在健康影響，如何降低作業人員暴露之可行性，實有進行探討之必要性。本研究擬建立雷射金屬沉積作業金屬燻煙微粒之特徵與逸散速率，並評估雷射金屬沉積作業勞工金屬燻煙微粒的暴露情形，且透過可接受之暴露風險的角度，提出LMD作業空間所需最保守估計之通風時間，來控管作業人員之進出，以達保護勞工健康之目的。

本研究以一設置一台機械手臂式雷射金屬沉積機台，及一提供100ACH的整體換氣系統之庫房(3.6m×3.8m×2.9m)為研究地點，使用SMPS於雷射沉積金屬機械手臂作業前之庫房內測量其背景濃度，再於庫房內使用上述直讀式儀器搭配MOUDI進行作業過程中微粒逸散的三重複採樣，以獲得之樣本再進行粒數、質量、表面積、重金屬濃度之逸散特徵分析，以微粒的數目、質量、表面積濃度為暴露評估指標並推估所需的通風時間以做為建立通風系統操作指引之基礎。

本研究結果顯示該作業產生之金屬燻煙微粒的數目濃度分布為雙峰型分布，其CMD為0.291 μm，0.029 μm，GSD為2.80和1.88，其質量濃度分佈也是雙峰型分布，MMAD分別為0.068 μm和15.5 μm，GSD分別為1.74和7.18，SMPS和APS的有效密度分別為0.13 g／cm3和0.35 g／cm3，且微粒沉積於肺泡區(AL)之比例皆遠大於頭區(HA)及氣管支氣管區(TB)。鎳的平均重金屬濃度為83.62 ± 36.19 μg／m3，95百分位值為161.07 μg／m3，超過短時間時量平均容許濃度（PEL-STEL = 50），且其總致癌風險（1.16×10-4）也不符合可接受標準值（10-6）。

因此，為控制勞工的金屬燻煙微粒暴露，故須採取適當的通風時間進行通風控制，由不同LMD操作時間與不同的可接受暴露評估指標進行通風時間之計算，發現由微粒數目、質量、表面積濃度和致癌風險所需的通風時間分別為13、10、10及7分鐘，從審慎的角度來看，LMD製程建議採用13分鐘的通風時間。

中 文 關 鍵 詞 ：雷射金屬沉積、金屬燻煙、暴露評估、控制策略

英 文 摘 要 ：Laser material deposition (LMD) technology is a method of depositing molten metal by irradiating a laser beam while ejecting metal powder to form a metal protective layer for anti-corrosion and anti-wear, or using the metal powder melt as the material for printing 3D objects. During LMD process is conducted, the laser power is set at 2000 watts (temperature : 1500 ℃ or higher), the metal powder was heated over the melting point and volatilized into the air,

then the metal vapor is aggregated at the ambient temperature to form the metal particles in a nanoparticle form. The present study was set out to investigate the emission characteristics of metal fume particles generated from the LMD process, then determined the suitable ventilation time for the LMD chamber to enter the LMD chamber to prevent workers from health hazards associated the emissions from the LMD process.

The studied LMD chamber (3.6m x 3.8m x 2.9m) is installed with a robot laser metal deposition machine and equipped with a general exhaust ventilation (GEV) system providing air exchange rate at 100 ACH. Direct-reading instruments of a SMPS and an APS were used to conduct sampling inside and outside the chamber to measure particle concentrations, and a MOUDI was used to conduct sampling inside to measure particle number and mass concentrations. Measurements conducted outside and inside were used to characterize the concentrations of the background and the LMD emissions, respectively. Samples collected by MOUDI were further analyzed for their heavy metal concentrations using ICP-MS. The resultant emission rates of the particle number, mass and surface area were used to determine the required ventilation time for different LMD time based on the acceptable level for different exposure metrics, which were served as a basis for establishing safety operating guidelines for the studied LMD process.

Results show that the number concentrations of metal fume emitted from the LMD process was in the form of the bimodal respectively with CMDs 0.291 μm, and 0.029 μm, and GSDs 2.80, and 1.88. The mass distribution of the emitted metal fume particles were also in a bimodal form, the MMADs 0.068 μm and 15.5 μm, and GSDs of 1.74 and 7.18, respectively. The fractions of the metal fume particles deposited on the alveolar region (AL) were much higher than that of other two regions (head airways (HA) and tracheobronchial (TB)). The mean workplace heavy metal concentrations for nickel was 83.62 ± 36.19 μg/m3, and 95%-tile level were 161.07μg/m3, which exceed the current exposure limits (PEL-STEL = 50) The resultant total cancer risk (CR) (1.16×10^{-4}) was also not comply with the acceptable value (10^{-6}). Hence, the use of ventilation system with adequate ventilation time is necessary for controlling workers' exposures to emitted metal fume particles. From the prudent aspect, the ventilation of 13 minutes is suggested for the LMD process. The present suggest a ventilation time of 13 minutes for the LMD process for a general exhaust system with 100 ACH.

英文關鍵詞：Laser metal deposition, metal fume, exposure assessment, control strategy

科技部補助專題研究計畫成果報告

（□期中進度報告/■期末報告）

（雷射金屬沉積作業人員奈米暴露評估控制指標之開發與應用）

計畫類別：■個別型計畫 　 □整合型計畫
計畫編號：MOST 　106－2221－E－040－001－
執行期間：106 年 8 月 1 日至 107 年 7 月 31 日

執行機構及系所：中山醫學大學 職業安全衛生學系

計畫主持人：王櫻芳
共同主持人：闕斌如
計畫參與人員：席珮瑄、蘇世心

本計畫除繳交成果報告外，另含下列出國報告，共 1 份：
□執行國際合作與移地研究心得報告
■出席國際學術會議心得報告
□出國參訪及考察心得報告

摘要

　　雷射金屬沉積作業(Laser Metal Deposition, LMD)列印技術已被廣泛應用於金屬模具、航太、鋼鐵、石化、機械五金等產業，該技術利用雷射能量讓同時間噴射出的金屬粉末材料熔融後覆蓋在母材上，並於母材上形成金屬保護層(抗腐蝕、抗磨耗、抗鏽蝕等)，或將金屬粉末熔融燒結後直接成型特殊造型體，而達到 3D 列印成型結構外形目的。雷射金屬沉積作業過程中，金屬粉末通過噴嘴自動施加，其所使用之雷射功率高達 2000 瓦之雷射源(溫度約 1500℃ 或更高)，透過雷射產生熔池，進行沉積作業。然而，其所使用之材料金屬粉末會因受熱超過熔點而揮發逸散到空氣中隨之因環境溫度而使金屬蒸氣膠結而形成氧化金屬微粒，呼吸暴露於金屬燻煙可能引起潛在健康影響，如何降低作業人員暴露之可行性，實有進行探討之必要性。本研究擬建立雷射金屬沉積作業金屬燻煙微粒之特徵與逸散速率，並評估雷射金屬沉積作業勞工金屬燻煙微粒的暴露情形，且透過可接受之暴露風險的角度，提出 LMD 作業空間所需最保守估計之通風時間，來控管作業人員之進出，以達保護勞工健康之目的。

　　本研究以一設置一台機械手臂式雷射金屬沉積機台，及一提供 100ACH 的整體換氣系統之庫房(3.6m× 3.8m × 2.9m)為研究地點，使用 SMPS 於雷射沉積金屬機械手臂作業前之庫房內測量其背景濃度，再於庫房內使用上述直讀式儀器搭配 MOUDI 進行作業過程中微粒逸散的三重複採樣，以獲得之樣本再進行粒數、質量、表面積、重金屬濃度之逸散特徵分析，以微粒的數目、質量、表面積濃度為暴露評估指標並推估所需的通風時間以做為建立通風系統操作指引之基礎。

　　本研究結果顯示該作業產生之金屬燻煙微粒的數目濃度分布為雙峰型分布，其 CMD 為 0.291 μm，0.029 μm，GSD 為 2.80 和 1.88，其質量濃度分佈也是雙峰型分布，MMAD 分別為 0.068 μm 和 15.5 μm，GSD 分別為 1.74 和 7.18，SMPS 和 APS 的有效密度分別為 0.13 g／cm³ 和 0.35 g／cm³，且微粒沉積於肺泡區(AL)之比例皆遠大於頭區(HA)及氣管支氣管區(TB)。鎳的平均重金屬濃度為 83.62 ± 36.19 μg／m³，95 百分位值為 161.07 μg／m³，超過短時間時量平均容許濃度（PEL-STEL＝50），且其總致癌風險（1.16×10⁻⁴）也不符合可接受標準值（10⁻⁶）。

　　因此，為控制勞工的金屬燻煙微粒暴露，故須採取適當的通風時間進行通風控制,由不同 LMD 操作時間與不同的可接受暴露評估指標進行通風時間之計算，發現由微粒數目、質量、表面積濃度和致癌風險所需的通風時間分別為 13、10、10 及 7 分鐘，從審慎的角度來看，LMD 製程建議採用 13 分鐘的通風時間。

關鍵字：雷射金屬沉積、金屬燻煙、暴露評估、控制策略

Abstract

Laser material deposition (LMD) technology has been widely used in metal mold, aerospace, steel, petrochemical, mechanical hardware and many other industries. LMD is a method of depositing molten metal by irradiating a laser beam while ejecting metal powder to form a metal protective layer for anti-corrosion and anti-wear, or using the metal powder melt as the material for printing 3D objects. During LMD process is conducted, the laser power is set at 2000 watts (temperature : 1500 ℃ or higher), the metal powder was heated over the melting point and volatilized into the air, then the metal vapor is aggregated at the ambient temperature to form the metal particles in a nanoparticle form. Inhalator exposures to these oxidized metals might encounter potential health hazards. The question regarding how to reduce the exposure dose of workers exposed becomes an important issue. The present study was set out to investigate the emission characteristics of metal fume particles generated from the LMD process, then determined the suitable ventilation time for the LMD chamber to enter the LMD chamber to prevent workers from health hazards associated the emissions from the LMD process.

The studied LMD chamber (3.6m × 3.8m × 2.9m) is installed with a robot laser metal deposition machine and equipped with a general exhaust ventilation (GEV) system providing air exchange rate at 100 ACH. Direct-reading instruments of a SMPS and an APS were used to conduct sampling inside and outside the chamber to measure particle concentrations, and a MOUDI was used to conduct sampling inside to measure particle number and mass concentrations. Measurements conducted outside and inside were used to characterize the concentrations of the background and the LMD emissions, respectively. Samples collected by MOUDI were further analyzed for their heavy metal concentrations using ICP-MS. The resultant emission rates of the particle number, mass and surface area were used to determine the required ventilation time for different LMD time based on the acceptable level for different exposure metrics, which were served as a basis for establishing safety operating guidelines for the studied LMD process.

Results show that the number concentrations of metal fume emitted from the LMD process was in the form of the bimodal respectively with CMDs 0.291 μm, and 0.029 μm, and GSDs 2.80, and 1.88. The mass distribution of the emitted metal fume particles were also in a bimodal form, the MMADs 0.068 μm and 15.5 μm, and GSDs of 1.74 and 7.18, respectively. The effective density for SMPS and APS were 0.13 g/cm^3 and 0.35 g/cm^3, respectively. The fractions of the metal fume particles deposited on the alveolar region (AL) were much higher than that of other two regions (head airways (HA) and tracheobronchial (TB)). The mean workplace heavy metal concentrations for nickel was 83.62 ± 36.19 μg/m^3, and 95%-tile level were

161.07μg/m^3, which exceed the current exposure limits (PEL-STEL = 50) The resultant total cancer risk (CR) (1.16 × 10^{-4}) was also not comply with the acceptable value (10^{-6}). Hence, the use of ventilation system with adequate ventilation time is necessary for controlling workers' exposures to emitted metal fume particles. Use the measured concentrations of different exposure metrics resulting from different LMD operating times and designated acceptable exposure levels, the required ventilation times for the particle number, mass, surface area concentrations and acceptable excessive cancer risk associated with heavy metal exposures were found to be 13, 10, 10 and 7 minutes, respectively. From the prudent aspect, the ventilation of 13 minutes is suggested for the LMD process.

Particles emitted from the LMD process were in the form of the bimodal show that the metal fumes contain nanoparticles and the fraction of particles deposited on the AL region was higher than that of the other two regions. The emitted heavy metal concentrations and the resultant health risks were found to be unacceptable. The present suggest a ventilation time of 13 minutes for the LMD process for a general exhaust system with 100 ACH.

Keywords: Laser metal deposition, metal fume, exposure assessment, control strategy

Introduction

The laser material deposition (LMD) technology has been widely used in metal mold, aerospace, steel, petrochemical, mechanical hardware and other industries, it is a method for depositing molten metal by irradiating a laser beam while ejecting metal powder to form a metal protective layer for anti-corrosion and anti-wear, or the metal powder melt and sintered until the 3D object is printed (Kyogoku 2014).

In the LMD process, the metal powder is automatically ejected through the nozzle, the laser power was set at 2000 watts (temperature: 1500 ℃ or higher), then the metal powder injected into the molt pool to form the deposition layer. However, the particle size of the metal powder is submicrometer, when the metal powder was heated over the melting point and volatilized into the air, the metal vapor is aggregated with the ambient temperature to form the metal particles which contain nanoparticles, respiration exposure to these metal oxidation are likely to occur metal fume fever, the symptoms include fever, chills, nausea, headache, fatigue, muscle aches, shortness of breath, pneumonia, chest pain, change in blood pressure, coughing, shock, convulsions, yellow eyes or yellow skin, rash, vomiting, and low or high blood pressure, etc. (McCann et al. 2002; Mueller and Seger 1985). Therefore, the LMD workers might encounter potential health hazards due to exposing to the metal fume particles, and how to reduce the dose of workers exposed is necessary for investigating.

At present, NIOSH also proposes the relevant specifications for worker exposure during the production or use of engineered nanomaterials. The employer should provide engineering controls to protect workers by removing hazards, for example, the local exhaust ventilation that captures and removes airborne emissions or placing a barrier between the worker and the hazard in the workplace (NIOSH 2014). Nanomaterials in workplaces should be encircled by enclosures and kept in a state of negative pressure such as glove boxes, chemical fume hoods, laminar table cabinets, and so on. If the process could not be enclosed, the local ventilation system is often used to control the nanomaterials emission.

Although the current the LMD chamber use the control method of the enclosure during the LMD operation, considering the air flow of the ventilation might impact the product quality during the LMD process, so the ventilation system will turn on after the whole LMD process is completed, and then the workers enter the LMD chamber to remove the product. At this time, the exposure risks of the contaminants and other residual materials are unknown, thus how long should ventilate is required to determine by establishing the relevant control metrics for decision making.

The potential toxicity of nanoparticles is related to its particle size, surface area, surface chemical, solubility, shape, and so on (Gatoo et al. 2014). Nanoparticles are

more harmful to health than large-sized particles because the extremely small size of nanoparticles leads them to be easily transported via inhalation to the pulmonary region of the lung (Donaldson et al. 1998; Maynard and Kuempel 2005; Oberdörster et al. 2005) And because of its large surface area, nanoparticle is much easier to react with metal, acidic or other organic substances (Oberdörster et al. 2005). On the other hand, because the physical and chemical property of the nanoparticle is different from the same materials at larger scales, the different levels of cytotoxicity depending on different particle size. However, it is reasonable to assess different exposure metrics of nanoparticle before the assessment index of the nanoparticle was not determined.

Objective

The present study was set out to investigate the emission characteristics of metal fume particles generated from the LMD process, and to determine the suitable ventilation time for the source enclosure ventilation installed in the LMD chamber based on the acceptable exposure risk for workers to enter the LMD chamber to prevent workers from health hazards during the LMD process.

Literature Review

(1) Laser metal deposition (LMD) process

Laser metal deposition (LMD) is one of additive manufacturing (AM) technologies. During the LMD process, a melt pool on the surface of the substrate or a previous layer is generated by high power laser radiation, simultaneously, the metal powder is injected into the melt pool by a powder feeding nozzle and melted completely. By moving the working table and/or the laser head, a metallurgical fused bonding is formed as shown in Fig. 1 (Zhong et al. 2016b).

LMD can clad, build, and rebuild components having complex geometries, sound material integrity and dimensional accuracy. Accordingly, LMD has a highly versatile process capability and can be applied to manufacture new components, to repair and rebuild worn or damaged components and to prepare wear and corrosion resistant coatings (Gu et al. 2012). Because of the various advantages of LMD such as low material waste, high production efficiency and high flexibility for especially individualized production, there has been a growing interest in its development in recent years in fields from process micro structure to mechanical properties and so on (Zhong et al. 2016a).

However, the commonly used powders for LMD are microparticles, there are numerous metal fumes would be generated in the LMD process which contains nanoparticles, and these particles will deposit within the respiratory system and injure the lung cells. That is, workers could expose to chemical and physical hazards

associated with the LMD process, wherefore it is important to prevent the occurrence of occupational diseases by working in the above-mentioned hazards.
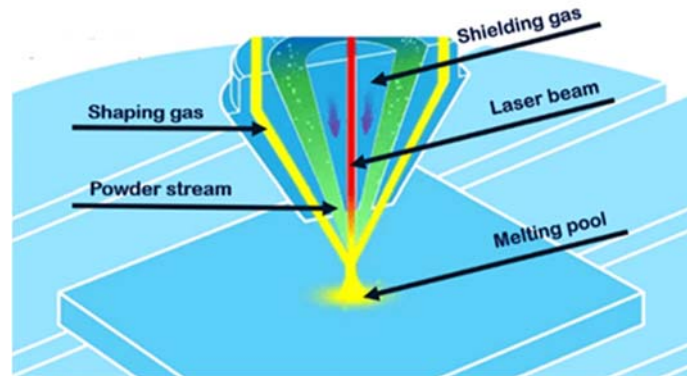

Figure 1 Schematic of LMD system

(2) Metal fume

Metal fume refers to a solid-particle produced by the condensation of vapors high-temperature heating products which suspended in air. These metal fume particles are often clusters or chains of primary particles, and the particle size range is from 0.02 to 2.5 μm normally (Gonser and Hogan 2011; Hinds 2012).

There are four main forms of metal fume particles, first, when the molten metal produces liquid metal, the metal alloy droplets begin to drain, causing small droplets to be forced away from the original metal droplets (Fig. 2a). Second, when the small metal droplets and oxygen form solid metal oxide particles(Fig. 2b); third, if the metal is heated then causes liquid metal to vaporize, it forms a smaller metal oxide particle with the oxygen in the air, that is, the metal oxide particles have been formed primary particles at the beginning (Figs. 2c, 2d). Fig.2 shows that the various methods of fume formation (Gray et al. 1983).

Because most of the metal fume contain submicrometer particles, it's easy to inhale those metal fume particles and may have effects on human body, especially occupational exposure to metal fume sometimes causes a chemical pneumonitis or even a lung cancer (Donaldson et al. 2005; Palmer et al. 2003).

On the other hand, extreme temperatures in the laser beam heat the metal powder to be joined the substrate which is made of metal pieces. The majority of the formed metal fume comes from the metal powder which is volatilized during the process. The vaporized metal becomes oxidized when it comes in contact with oxygen in the air, producing metal oxides which condense and form respirable-sized fume which is likely to be deposited in the alveolar regions of the lungs (Antonini et al. 2003).
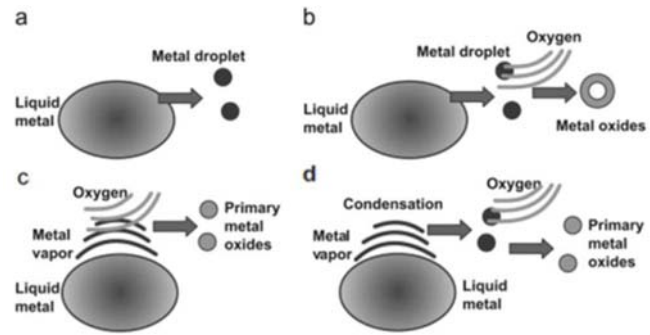
Figure 2 Metal fume particles formation mechanism (Gray et al. 1983)

(3) Current metal fume exposure to laser process

Most of the relevant literature of laser metal fume is laser metal cutting operations, although the operating type is different, the mechanisms for the generation of metal fume are the similar. Therefore, we reviewed the literature which is about exposure to laser cutting.

Barcikowski et al. (2007) examined femtosecond laser ablation in air in order to study the properties of nanoparticles that are obtained in typical conditions of femtosecond laser micromachining applications, and found 90% of the metal fume particles produced by CO_2 laser ablation of titanium and ferric alloys in air are smaller than 1 μm (aerodynamic diameter). And the smallest single particles have geometric diameters of about 5 nm to 10 nm.

Elihn et al. (2009) examined the metal fume nanoparticles area exposure in a plant which includes laser cutting and welding of steel. They found the total particle number concentration of 80000 #/cm^3 was measured at laser cutting, and the GMD is 450 nm, the GSD is 2.2, the surface area is 3800 μm^2/cm^3. At laser cutting, especially large particles and surface area concentrations were found, compared to those at the other work activities. At these hot processes, the particle concentrations were generally higher compared to those at colder processes (Elihn and Berg 2009).

Chiung et al. collected the environmental samples in the laser cutting workplace to analyze the distributions of different particle size. The results showed that the use of different metal materials in the laser cutting processes might influence the metal fume nanoparticle characteristics, and from the observation of all measures under different laser cutting models, they found the concentration of nanoparticles was associated with the laser cutting power in femtosecond laser operation.

The energy used in the drilling of the steel sheet is the highest in femtosecond laser operation, and the average particle number concentration is about 20000 - 3000 #/cm^3. The energy of the thin steel sheet is smaller, and the average particle number concentration is about 10000 - 2500 #/cm^3, and the nanoparticles emitted from the femtosecond laser cutting process was in the form of the unimodal with MMAD and GSD as 250 nm and 1.75, respectively.

During CO_2 laser cutting operation, it was related to the materials used and incises power. The particle size distribution of the copper particles, aluminum sheets and stainless steel was 92 nm, 102 nm and 64 nm, and the GSD was 1.91, 1.45 and 2.33, respectively, also the above-mentioned were unimodal. However, the particle size distribution of carbon steel was bimodal, the NMDs were 25 nm and 98 nm, the GSDs were 1.65 and 1.93. The results of NMDs showed that the particles generated from CO_2 laser processing of stainless steel and carbon steel were nanoparticles. At the whole CO_2 laser cutting process, the MMAD and GSD were 544 nm and 2.93, respectively.

(4) Emission rate of nanoparticle

The emission rates of nanoparticles for different operations and theirs results are summarized in Table 1, including candle-burning, cooking activities, vehicle operation, welding operations and so on, since there is no emission rate for laser metal deposition operation can be referred to today.

The laser source with a maximum output power of 2 kW (temperature: 1500 ℃ or higher), and the metal powders for LMD are microparticles, it is easy for metal fume generated. Although the operation process is under enclosure conditions, after the coating is finished, the worker will expose to the metal fume particles when he/she enters the chamber to carry out the product. Therefore, it is important and necessary to investigate how to determine the ventilation time of the chamber to reduce the exposure to workers.

Table 1 Summary of emission rates of nanoparticles

Source	Description of burn mode/activity	Measured size range	Emission rate	Emission factor	Reference
Candle (Paraffin)	Steady burn	10-500 nm	2.45×10^{13} (#/h)	4.05×10^{12} (#/g)	(Zai et al. 2006)
	Unsteady burn		1.05×10^{13} (#/h)	1.49×10^{12} (#/g)	
	smoldering		1.55×10^{13} (#/h)	-	
Candle	Steady burn	16-1000 nm	0.9—25.3 (mg/h)	-	(Pagels et al. 2009)
Cooking	Gas stove at full power	< 100 nm	2.1×10^{12} (#/min)	-	(Buonanno et al. 2009)
	Grilling with gas stove at full power		3.0×10^{12} (#/min)	-	
	Grilling with gas stove at minimum power		1.2×10^{11} (#/min)	-	
	Grilling with electric stove at maximum power		1.3×10^{12} (#/min)	-	
	Grilling with electric stove at minimum power		2.9×10^{11} (#/min)	-	
Traffic exhaust	Diesel car	25-400 nm	-	$1.1—2.7 \times 10^{14}$ km^{-1}	(Wehner et al. 2009)
	Gasoline car		-	$0.6—3.5 \times 10^{12}$ km^{-1}	
Automotive plant	Welding	5.6-560 nm	2.8×10^{15} (#/min)	-	(Buonanno et al. 2011)
Indoor combustion	Paraffin wax candle	0.006-20 μm	4.85×10^{13} (#/h)	1.30×10^{12} (#/g)	(Stabile et al. 2012)
	Natural corn wax candle		4.07×10^{13} (#/h)	1.82×10^{12} (#/g)	
	Mosquito coil		4.57×10^{14} (#/h)	1.41×10^{12} (#/g)	
	Citronella stick		2.92×10^{14} (#/h)	1.16×10^{12} (#/g)	
3D printer	Filament of ABS	11.5-116 nm	9.7×10^{10} (#/min)	-	(Stephens et al. 2013)
	Filament of PLA		2.0×10^{10} (#/min)		
3D printer	Filament of ABS	10-420 nm	1.61×10^{10} (#/min)	1.67×10^{11} (#/g)	(Kim et al. 2015)
	Filament of PLA1		4.89×10^{8} (#/min)	3.77×10^{9} (#/g)	
	Filament of PLA2		4.27×10^{8} (#/min)	3.91×10^{9} (#/g)	
3D printer	Filament	10-1000 nm	$2 \times 10^{8} \sim 4 \times 10^{10}$ (#/min)	-	(Azimi et al. 2016)

(5) Metal fume particles hazard control

    Metal fume particles have been linked to several detrimental acute and chronic health effects, one reason probably due to exposure to metal fume particles with compositions of chemicals (Lee et al. 2006). Fig. 3 illustrates the hierarchy of hazard controls, the hierarchy provides five preference rankings for hazard controls, the bottom tiers tend to be the least effective, while the top tiers are the most effective (NIOSH 2016). If the potential hazard cannot be eliminated, then engineering controls should be installed and tailored to the process or job task. Engineering control techniques such as source enclosure and local exhaust ventilation systems could be effective for capturing airborne metal fume particles (Schulte et al. 2008), a summary of the control techniques for exposure control of nanoparticles together with comments is given in Table 2.
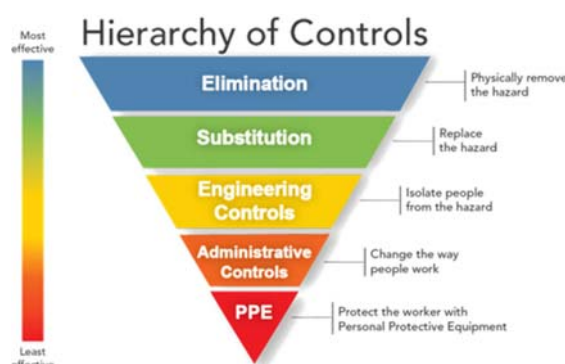

Figure 3 The hierarchy of hazard controls

Table 2 The control techniques for exposure control of metal fume particles

Material	Process	Control used	Exposure without control	Exposure with control	Relevant bilk OEL	Reference
Welding fume	Arc welding	Booth	7.78×10^5 p/cm^3	1.48×10^4 p/cm^3		(Lee et al. 2006)
Welding fume	Steel welding	Portable local exhaust ventilation	4.95 mg/m^3	4.47 mg/m^3	5 mg/m^3 (Total fume)	(Meeker et al. 2007)
Carbon nanotubes	Blending for composites	Enclosure	172.9 f/ml – 193.6 f/ml	0.018 f/ml – 0.05 f/ml		(Han et al. 2008)
Nanomaterial	Gas phase manufacturing	Enclosure		0.188 mg/m^3 (Steady state with process operating)	3 mg/m^3	(Demou et al. 2008)
Nanomaterial	Gas phase manufacturing	Enclosure		59100 p/cm^3 (Steady state with process operating)		(Demou et al. 2008)
Nanomaterial (insoluble and soluble, many types)	Nanoparticle production by flame spray pyrolysis	Fume hood with extraction		0.037 mg/m^3 PM1 (max) (differentiated from background)	3 mg/m^3	(Demou et al. 2009)
Nanomaterial (insoluble and soluble, many types)	Nanoparticle production by flame spray pyrolysis	Fume hood with extraction		10000 p/cm^3 (Steady state with process operating)		(Demou et al. 2009)
Nano-alumina	Pouring/ transferring of nanomaterial	Fume hood with extraction		1575 p/cm^3 – 13260 p/cm^3		(Tsai et al. 2010)

Materials and Methods

(1) Sampling site

The laser processes are done in the LMD chamber which is installed with a robot laser metal deposition machine and equipped with a ventilation system as shown in Fig. 4. The studied LMD chamber (3.6m × 3.8m × 2.9m) with four exhaust ports (29cm × 29 cm) located four corners of the wall, three fresh air inlets (22cm × 42 cm) placed at the door, and set at 100 air changes per hour (ACH).

The laser power of the robot laser metal deposition machine was set at 2 kW, the scan speed was set at 10mm/s, and the fiber core diameters was 400 μm, an apparatus with a 304 stainless steel substrate (20cm × 20cm) to assist with laser metal deposition process.

Direct-reading instrument of a scanning mobility particle sizer (SMPS) and an aerodynamic particle sizer (APS) were used to conduct sampling inside and outside the chamber to measure the background particle concentrations for 2 hours, then with a microorifice uniform deposit impactor (MOUDI) to measure the particle concentration inside the chamber during the LMD process, each sampling was conducted for 6 minutes to measure particle number and mass concentrations and tested for three times, the former 5 minutes was the laser metal deposition operation time, and the latter 1 minute was the time of machine adjustment. The SMPS, APS and MOUDI were positioned as close as possible to the particle emission source as possible which were shown in Fig. 5.
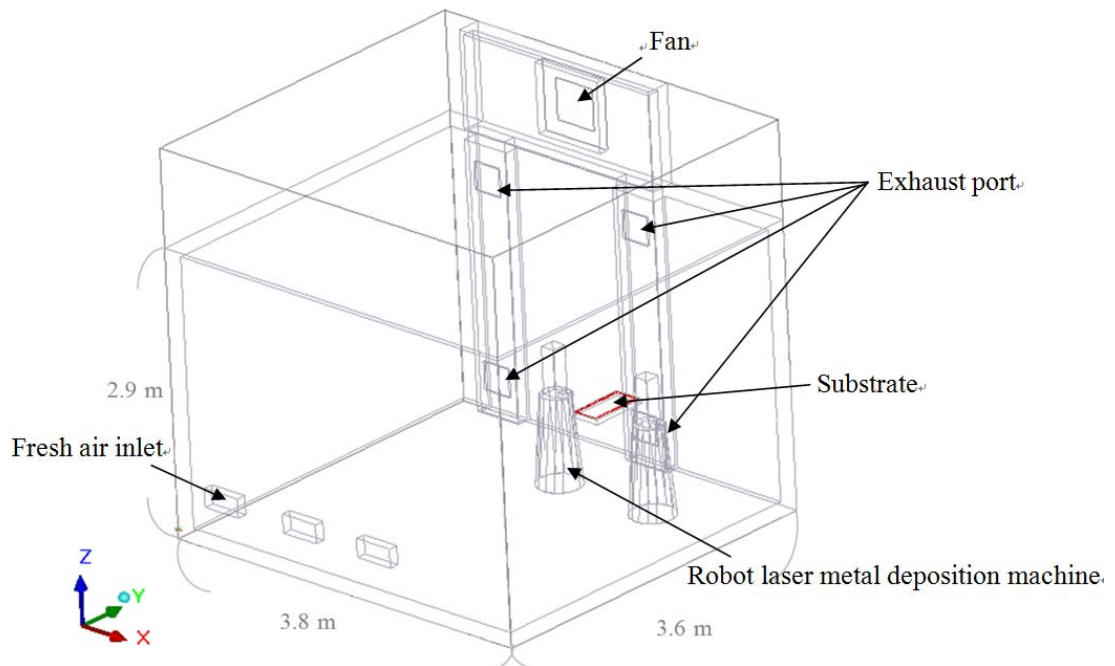

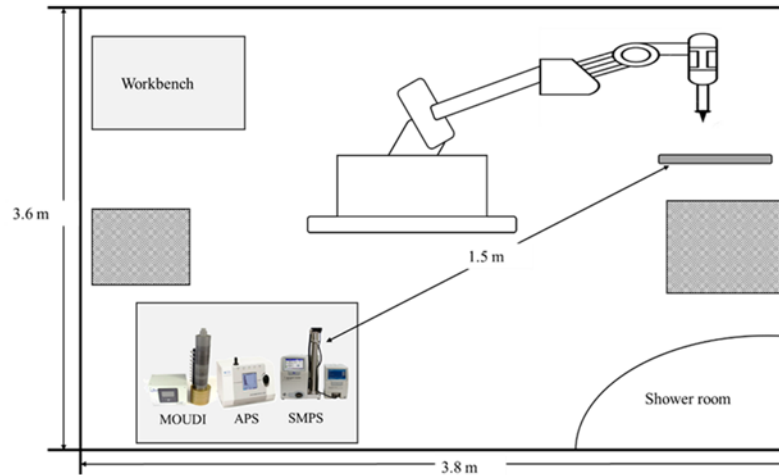Figure 4 Schematic diagram of the sampling site

Figure 5 Schematic diagram of the sampling instruments in the LMD chamber

(2) Powder materials

The used powder was the spherical nickel alloy, also known as IN718 powder, with the particle diameter <1 mm, and the melting range from 1350 to 1450 °C, which is well suited for applications requiring high strength and high creep-rupture resistance. IN718 also exhibits excellent tensile and impact strength, so it is widely used in the field of aircraft industries (Zhong et al. 2016a), the main chemical compositions of the used powder have been listed in Table 3.

Table 3 Chemical compositions of IN718 powder (in weight percent, wt %)

Ni	Cr
50 - 70%	10 - 25%

(3) Sampling instruments and methods

A. MOUDI

MOUDI (Micro-Orifice Uniform Deposit Impactor, Model 122R, MSP Co., Minneapolis, MN, USA) is a ten-stage cascade impactor, with cut-sizes ranging from 0.056 to 18 μm at a flow rate of 30 L/min.

The principle of operation is a jet of particle-laden air is directed at a flat impaction plate, the larger are collected on the plate while the smaller follow the airflow out of the impaction region and are not collected. MOUDI is easy to collect particles in discrete size ranges by passing the aerosol through a number of stages which is one stage consisting of a nozzle and impaction plate in series, with each subsequent stage collecting particles smaller than the one before it (Marple et al. 1991).

MOUDI has the cut-off aerodynamic diameter of 18, 10, 5.6, 3.2, 1.8, 1.0, 0.56, 0.32, 0.18, 0.10, 0.056 μm and the after filter of ＜0.056 μm, so it can measure mass concentration distribution of particles.

12

For gravimetric analysis, aluminum foils (47mm, Diamond Corp., USA) which were coated silicone grease (KF96SP, Shin-Etsu Chemical Co., Japan) were used as the impaction substrates from the inlet to the 10th stages to reduce solid particle bounce, and Teflon filter (PTU109010, STERLITECH Corp., USA) was used on the 11th stage that is after filter. For heavy metal analysis, the substrates from the inlet to the 10th stages were Teflon filters (Zefluor P5PJ047, Pall Corp., New York, USA), and the last stage was the same as gravimetric analysis which was Teflon filter (PTU109010, STERLITECH Corp., USA).

B. SMPS

SMPS (Scanning Mobility Particle Sizer, Model 3082, TSI Inc., St. Paul, MN, USA) is able to measure the size distribution and concentration of particle in the size of 1 nm to 1 μm which is based on the physical principle that the ability of a particle to traverse an electric field with the aim of removing excess particles, then the particles will be charged to form a Bozeman distribution, when the charged particles is in the Boltzmann distribution, then into the DMA. In a DMA (Differential Mobility Analyzer), an electric field is created and the airborne particles drift in the DMA according to their electrical mobility. Particle size is then calculated from the mobility distribution. And the followed particles will enter the CPC (Condensation Particle Counter) to calculate the number of particles. CPC is a particle counter that detects and counts aerosol particles by first enlarging them by using the particles as nucleation centers to create droplets in a supersaturated gas. At this time, the periphery of the particles will grow with a layer of liquid, then measure the number of particles by a photodetector, the detection limit concentration range up to 10^7 #/cm^3.

The SMPS which was set to measure particle size distribution and number concentration, in the range from 10.9 to 371.8 nm, sheath flowrate is 6 L/min, aerosol flowrate is 0.599 L/min, the scan time is 170 seconds, and the retrace time is 3 seconds.

C. APS

APS (Aerodynamic Particle Sizer, APS, Model 3321, TSI Inc., St. Paul, MN, USA) is based on aerodynamic behavior, determining the particle size by using a time-of-flight (TOF) method. In accelerated flow field, the time taken from the particle to pass between two parallel laser beams is measured. The resulting particle acceleration rate is converted to a corresponding aerodynamic diameter, which is defined as a particle that has the same settling speed than a spherical particle with the density of 1 g/cm^3, the larger the acceleration in the flow field is, the smaller the size of the particle will be, and the larger size of the particle is just the opposite. The particle size distribution can be obtained by measuring the number of particles and the aerodynamic diameters of the particles, the particle size measuring ranges by APS

from 0.542 to 19.81 μm, the aerosol and sheath flow rates are 1 and 4 L per minute, respectively, and the sample time is 180 seconds.

However, APS is not suitable for the determination of high concentrations of particles (the limit of detection concentration range is 10^4 #/cm^3). When too many particles enter into APS at the same time, may lead to an erroneous detection which is so-called coincidence error, it is mistaken the multiple particles for a single particle of larger size, resulting in phantom particles and underestimation of number counts (Peters and Leith 2003).

D. Air velocity meter

Air velocity meter (Velocicalc air velocity meter, 9565-X, TSI Inc., St. Paul, MN, USA) can simultaneously measures and data logs several ventilation parameters using a single probe with multiple sensors. It measures velocity, temperature, and relative humidity. The air velocity ranges between 0 and 30 m/s, and the temperature and relative humidity of the LMD chamber were 25 ± 1 °C and 70 ± 10 %, respectively. The air velocity measurements were taken 12 points for each vertical plane and there were 4 vertical planes (0.45, 1.35, 2.25, and 3.15 m) for the LMD chamber.

(4) Sample analysis

A. Mass concentrations

The aluminum substrates and Teflon filters were conditioned at 20±1 ℃ and relative humidity of 40±5 % for 24 hours before and after sampling. A microbalance (XP6, Mettler-Toledo, USA) was used to determine particle mass, the ambient temperature maintained at 20±1 ℃, and the relative humidity remained at 40 ± 5% in the weighing room. Discharge the filters before weighing by using the anti-static kit to avoid electrostatic charging which will cause adverse effects on weighing. Each filter must weigh at least three times, and the weight of Teflon filter should fall within ± 2 μg of expected value, and so does the aluminum foil. After weighing, the filters were sealed by using zip lock bags and stored in the refrigerator at 4 ℃.

B. Heavy metal content concentrations

The samples collected by the Teflon filters were digested by a micro oven before chemical analysis. Afterwards, these filters were analyzed using an ICP-MS (Inductively Coupled Plasma Mass Spectrometry, ICP-MS, Agilent 7700x, UK) based on the USEPA SW-846 chapter 3: inorganic analyses (USEPA 2014). The heavy metal content concentration analysis of this study, the collected samples must be pre-treated by microwave digestion, the method is a microwave digestion furnace with high pressure and temperature through microwave irradiation, the detailed microwave digestion procedures are as follows:

i. Add a few drops of deionized water to each vessel prior to taring to pre-wet the analytical portion.

ii. A minimum of 2 MBKs (method blanks) and must be included in each digestion batch to verify the absence of contamination that may arise from the vessels, add 5 mL of 4% HNO_3 solution for each MBK.

iii. Use 5 mL of 4% HNO_3 solution for each field blank sample (2 field blank samples in each digestion batch) and each sample of unknown composition.

iv. Add 5 mL of 65% HNO_3 solution and 0.3 mL of 40% HF solution to each vessel, washing down any material on walls, seal vessels and let the vessels sit in a clean hood for 30 minutes.

v. Run the stage1 of the digestion program in Table 4.

vi. Move vessels to an exhausting clean hood and vent excess pressure slowly, let uncovered vessels cool for 30 minutes.

vii. After vessels have cooled, add 2.8 mL of 5% H_3BO_3 solution to each vessel, let the vessels (uncovered) sit in a clean hood for 10 minutes.

viii. Run the stage2 of the digestion program in Table 4.

ix. Move vessels to an exhausting clean hood and vent excess pressure slowly, let uncovered vessels cool for 30 minutes.

x. Transfer each digest to a clean container and dilute digestion solution to approximately 15 mL with 1% HNO_3 solution.

Table 4 Digestive system conditions

Stage 1		
Power (W)	Ramp (min)	Hold (min)
400	5	5
500	5	5
600	5	20
0	-	20
Stage 2		
Power (W)	Ramp (min)	Hold (min)
600	20	10
0	-	15

The quality assurance/quality control (QA/QC) process for analytical methods, procedures, and controls should serve to enhance the probability that representative samples are collected and that the analytical results accurately describe the quality of the heavy metal concentrations from filters.

i. Initial calibration (IC): analyze nine calibration levels with a correlation factor (R^2) greater than or equal to 0.995.

ii. Initial calibration verification (ICV): analyze the initial calibration verification immediately after the IC. The recovery criteria would be within 90-110%.

iii. Initial calibration blank (ICB): analyze the initial calibration blank immediately after the ICV and prior to analysis of the high standard

verification. The analytes must be at levels below the method detection limit (MDL).

iv. Continuing calibration verification (CCV): analyze a mid-range calibration standard after every 10 sample analyses to verify the IC. The recovery criteria would be within 90-110%.

v. Continuing calibration blanks (CCB): analyze a CCB immediately following each CCV. The analytes would be at levels below the MDL.

vi. Method spikes and method spike duplicates: analyze one method spike and one method spike duplicate per batch of samples to determine that the matrix effects from the filters at a frequency of one per batch of samples prepped.

vii. Method blanks (MB): analyze a method blank for every 20 sample analyses. The MB contains all the reagents in the sample preparation procedure and must be prepared and analyzed as a sample to determine the background levels from the instrument. The analytes would be at levels below the MDL.

viii. Matrix spikes (MS): analyze one matrix spike per batch of samples at 1 per 20 samples, to determine the matrix effects from the filter. The recovery criteria would be within 75-125%.

ix. Laboratory control spike (LCS): a laboratory control spike must be prepared from a secondary source of calibration standards and analyzed with each sample batch. The recovery criteria would be within 80-120%.

x. Internal standards (IS): the intensities of all internal standards must be monitored for every analysis.

xi. Serial dilution (SD): the ICP serial dilution analysis must be performed on one sample per batch. After a fivefold serial dilution, the analyte concentration would be within 90 and 110% of the undiluted sample results.

xii. Rinse blank (RB): flush the system between standards and samples with 2% nitric acid in DI water.

Heavy metal concentration in the air sample should be calculated as follows:

$$C = (C_{ana} \times V_{dig}) / V_{std} \tag{1}$$

where C is the heavy metal concentration (g/m^3); Cana is the analyte concentration (g/L); Vdig is the filter extract volume (L/filter); Vstd is the sampling air volume (m^3).

(5) Data analysis

A. **Particle concentrations and size distribution**

In order to merge the particle mass concentration distribution obtained by SMPS, APS and MOUDI, the conversion formula used for each concentration interval is

shown by the Eq. 2 and 3. (Khlystov et al. 2004):

$$C_{Mi} = C_{Ni} \times \frac{\pi}{6} D_{Pi}^3 \times \rho_{Pi} \times 10^{-15} \quad for \ SMPS \tag{2}$$

$$= C_{Ni} \times \frac{\pi}{6} \frac{D_{Pi}^3}{\sqrt{\rho_{Pi}}} \times 10^{-15} \quad for \ APS \tag{3}$$

B.   Particle concentrations deposited in the respiratory tract

Assuming that the particle size distribution is represented well by a log-normal distribution, it should be possible to estimate the three parameters characterizing it: count median diameter (CMD), geometric standard deviation (σ_g) and total concentration, using just three independent measurements (Maynard 2003).

In this study, the results of the particle size distribution obtained by the direct-reading instrument were used to estimate the particle surface area according to the theoretical formula developed by Maynard (2003). The theoretical formula is shown in Eq. 4 and Eq. 5. First, substituting the CMD, the GSD, and the total particle concentration (N) into Eq. 4 and Eq. 5 to obtain the total particle surface area (S). Second, converting the CMD to the surface area median diameter (SMD), the conversion equation is given by Eq. 6, and finally, the total surface area concentration obtained by the Eq. 4 is multiplied by the surface area concentration distribution ratio of each particle size interval and the ICRP deposition fraction of each region (Eq. 8 – Eq. 11), as shown in the Eq. 7 (Hinds 2012).

$$S = N\pi d_{\bar{s}}^2 \tag{4}$$

$$d_{\bar{s}} = CMD \exp\left(\ln^2 \sigma_g\right) \tag{5}$$

$$SMD = CMD \exp(2\ln^2\sigma_g) \tag{6}$$

$$df = \frac{1}{\sqrt{2\pi}\ln\sigma_g} \exp(-\frac{(\ln d_p - \ln SMD)^2}{2(\ln \sigma_g)^2})d \ln d_p \tag{7}$$

where S is the total surface area concentration ($\mu m^2/cm^3$); N is the total number concentration ($\#/cm^3$); $d_{\bar{s}}$ is the average surface area diameter (μm); CMD is the count median diameter (μm); SMD is the surface area median diameter (μm); σ_g is the geometric standard deviation; df is the fraction of surface area concentration distribution; dp is the aerodynamic diameter of the particle.

The International Commission on Radiological Protection (ICRP) developed a model to predict particle deposition in different regions of the human respiratory tract

(ICRP 1994). The model covers various breathing characteristics and particle sizes from 1 nm to 100 μm. According to the ICRP Task Group Lung Model and based on Hinds' parameterization, gender and activity-weighted average deposition efficiency curves from the ICRP model were widely used to assess the depositions of nanoparticles in the respiratory tract on both number and mass concentration basis. The following equations (Hinds 2012) describe the grand average deposition distribution efficiency curves of the ICRP model for nasal breathing. For each region of the respiratory tract, the model gives the deposition efficiency as a ratio of the total airborne concentration.

$$DF_{HA} = IF\left(\frac{1}{1+\exp(6.84+1.183\ln d_p)} + \frac{1}{1+\exp(0.924-1.885\ln d_p)}\right) \tag{8}$$

$$DF_{TB} = \left(\frac{0.00352}{d_p}\right)\left[\exp(-0.234(\ln d_p+3.40)^2)+63.9\exp(-0.819(\ln d_p-1.61)^2)\right] \tag{9}$$

$$DF_{AL} = \left(\frac{0.0155}{d_p}\right)\left[\exp(-0.416(\ln d_p+2.84)^2)+19.11\exp(-0.482(\ln d_p-1.362)^2)\right] \tag{10}$$

$$IF = 1-0.5\left(1-\frac{1}{1+0.00076d_p^{2.8}}\right) \tag{11}$$

where d_p is the aerodynamic diameter of the particle; DF_{HA} is the deposition fraction for the head airways region; DF_{TB} is the deposition fraction for the tracheobronchial region; DF_{AL} is the deposition fraction for the alveolar region; IF is the inhalable fraction according to ICRP model.

C. Emission rates and factors

In order to estimate the particle emission rates during LMD operation, the following equation was used (Kim et al. 2015).

$$C_{cor} = C_d - C_b \tag{12}$$

$$P_{in\ the\ SMPS} = C_{cor} \times \text{sampling flow rate of SMPS} \times 1000 \tag{13}$$

$$ER = \frac{\text{total sampling flow rate} \times P_{in\ the\ SMPS}}{\text{sampling flow rate of SMPS}} \tag{14}$$

$$EF = \frac{ER \times t_{sampling}}{W_{powder}} \tag{15}$$

where C_{cor} is the correction of before operation concentration (#/cm^3); C_d is the during operation concentration (#/cm^3); C_b is the before operation concentration (#/cm^3); $P_{in\ the\ SMPS}$ is the emission rate of SMPS (#/min); ER is the total emission rate (#/min); EF is the total emission factor; $t_{sampling}$ is the sampling time; W_{powder} is the weight of the used powder.

D. Health risk assessment

For carcinogens, the lifetime average daily dose (ADD) used in the assessment of cancer risk has been calculated as a weighted average as shown in Eq. 16.

Calculation of the lifetime average daily dose for carcinogens (Ferreira-Baptista and De Miguel 2005):

$$ADD = \frac{C \times IR \times ET \times EF \times ED}{BW \times AT} \tag{16}$$

where C is the containment concentration (mg/m³); IR is the intake rate (m³/hr); ET is daily exposure times (hrs/day); EF is the exposure frequency (days/year); ED is the lifetime exposure (years); BW is the body weight (kg); AT is the life expectancy (years), all parameters used in the equations are defined in Table 5 .

Table 5 Exposure parameters for the health risk assessment

Parameter	Description	Exposure value	Units	Comment
C	containment concentration	environmental monitoring data	mg/ m³	
IR	intake rate	0.76	m³/day	
ET	daily exposure time	0.42	hr/day	One run required 5 minutes, and the worker will operate the LMD machine 5 times per day.
EF	exposure frequency	250	day/year	
ED	exposure duration	3	year	The workplace is the test site, the development period of the LMD machine is about 3 years.
BW	body weight	70	kg	
AT	average time	80.2	year	

Conducting a traditional deterministic risk assessment was to estimate potential cancer risks associated with inhalation exposures to metal fumes in the air for workers, and the equations are shown in below (USEPA 2009):

$$Cancer\ risk = ADD \times CSF \tag{17}$$

where CSF is the cancer slope factor ((mg/kg-day)⁻¹), the CSF of nickel and chromium (VI) are 0.91 (mg/kg-day)⁻¹ and 510 (mg/kg-day)⁻¹, respectively.

And when exposed to a variety of carcinogenic substances, assuming that there is no synergistic and antagonism effect, so the carcinogenic risk is the sum of all risks:

$$Risk\ T = \sum Risk\ I \tag{18}$$

where RISK T is the sum of all risks of carcinogenic and Risk I is the cancer risk of carcinogenic substance I.

E. Ventilation time of particle

The following equation was used to estimate particle decay rates due to penetration and deposition, following a source event (assuming no particle generation or coagulation during decay) (Howard-Reed et al. 2003):

$$\frac{dC_{int}}{dt} = P_p a C_{out,p} - a C_{int} - K_p C_{int} \tag{19}$$

where C_{int} is initial indoor particle concentration ($\#/m^3$); $C_{out,p}$ is the outdoor particle concentration for specific particle size p; t is time unit (h); P_p is the penetration coefficient for specific particle size p (dimensionless); a is the air change rate (1/h); K_p is the deposition loss rate coefficient for specific particle size p describing losses to room surfaces (1/h). Although the C_{int} and $C_{out,p}$ are expressed in terms of number concentration, it can also convert the unit of Eq. 20 from number to mass or surface area concentration.

The deposition rate of particles is related to particle concentration C_{int} by a deposition coefficient, K_p, through

$$\frac{dC_{int}}{dt} = -K_p C_{int} \tag{20}$$

Mathematically, the value of K_p is the sum of $K_{p,w}$, $K_{p,c}$, and $K_{p,f}$, which represent the deposition coefficients for wall, ceiling, and floor, respectively.

$$K_{p,w} = \frac{2S_w}{\pi V} \sqrt{DK_e} \tag{21}$$

$$K_{p,c} = \frac{S_c}{V} \frac{v_s}{\exp(\frac{\pi}{2} \frac{v_s}{\sqrt{DK_e}}) - 1} \tag{22}$$

$$K_{p,f} = \frac{S_f}{V} \frac{v_s}{1 - \exp(-\frac{\pi}{2} \frac{v_s}{\sqrt{DK_e}})} \tag{23}$$

where S_j is the respective area of the jth surface (m^2); V is the room volume (m^3); D is particle diffusivity (cm^2/s); Ke is the turbulence intensity (1/s).

The turbulence intensity, Ke, can be determined from the flow velocity gradient which is a function of average flow velocity, u, and the length of the surface in the direction of flow, L, by

$$K_e = K_o^2 \frac{du}{dx} \tag{24}$$

where x is the distance from the surface; du/dx is the flow velocity gradient (1/s); K_o is the Karman turbulence constant.

The velocity gradient in above equation is given by (Xu et al. 1994)

$$\frac{du}{dx} = 0.037(\frac{u^9\rho^4}{\eta^4 L})^{\frac{1}{5}}$$

(25)

where ρ is the air density (g/cm^3) and η is air viscosity (g/cm-s).

The penetration coefficient, P_p, could be found after obtaining the deposition rate which is shown as follows (Chao et al. 2003):

$$P_p = (1 + \frac{-K_p C_{int}}{a})\frac{C_{ss}}{C_{out,p}}$$

(26)

where Css,p is steady-state indoor particle concentration (#/m^3).

Result and Discussion

(1). Particle size distributions of particles from the LMD process

The particle number size distribution of the metal fume particles with background was in the form of the bimodal with count median diameters (CMDs) and geometric standard deviations (GSDs) as 0.291 μm, 0.029 μm and 2.80, 1.88, respectively, as shown in Fig.6.

The background particle number size distribution is shown in Fig. 7 and Fig. 8 is the particle number size distribution with no background, we found there were only 0.002% of the particle number concentrations came from the data of APS, it seems that the particle number concentrations measured by APS are meaningless, therefore, the following results of particle number concentrations would be interpreted by the data from SMPS only.

Fig. 9 shows the particle mass distribution of metal fume particle was bimodal, the mass median aerodynamic diameters (MMADs) were 0.068 μm and 15.5 μm with GSDs of 1.74 and 7.18, respectively; Fig. 10 shows the particle surface area distribution of metal fume particle, the surface area median diameter (SMD) was 0.045 μm with GSD of 1.74. The results of CMD, MMAD, and SMD showed that most of the particles generated from the LMD process were nanoparticles.
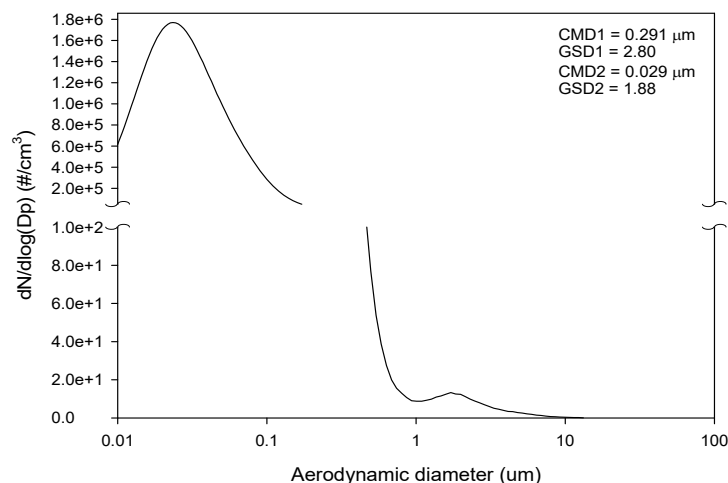
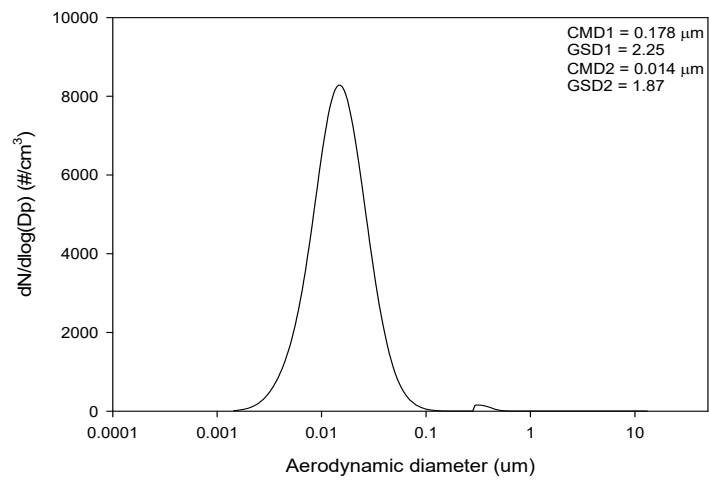Figure 6 Particle number size distribution of metal fume particles from the LMD process

Figure 7 Background particle number size distribution in the LMD chamber
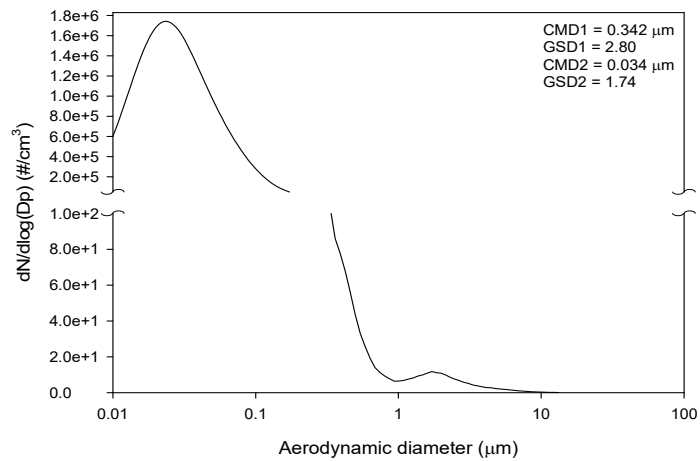

Figure 8 Particle number size distribution with no background
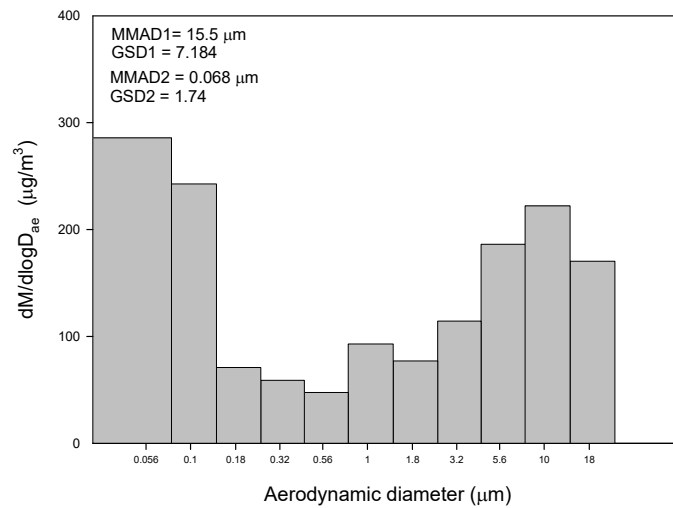
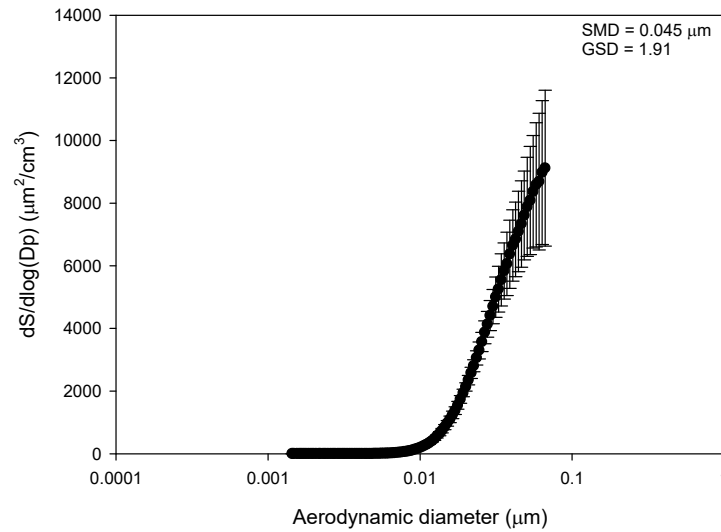Figure 9 Particle mass distribution measured by MOUDI

Figure 10 Particle surface area size distribution of metal fume particles from the LMD

(2). Predicted regional particle depositions of metal fume particles from the LMD process

To investigate current workplace exposure can use particle number concentrations to estimate exposure in terms of regional particle depositions. The advantage of this is that we can use the currently available methods, so we have little or no additional work to do while collecting exposure data. The measurement results could be interpreted as giving a very approximate estimate of the deposition fraction, reveal the possibility of associating health effects with different metrics, such as number, mass, and surface area, provide supportive evidence for this study into different exposure metrics and assessment methods, therefore, we estimated the regional particle depositions of metal fume particles as listed in Table 6.

The results showed the estimated number, mass, and surface area concentrations deposited on the three regions of the head airways (HA), tracheobronchial (TB), and alveolar (AL) of the respiratory tract. For the number concentrations, the estimated concentrations for the HA, TB, and AL regions were 1.73×10^5 #/cm^3, 2.38×10^5 #/cm^3, and 5.72×10^5 #/cm^3, respectively. For the mass concentrations, the estimated concentrations for the HA, TB, and AL regions were 8.77×10^{-8} μg/cm^3, 1.54×10^{-7} μg/cm^3, and 5.91×10^{-7} μg/cm^3, respectively. For the surface area concentrations, the estimated concentrations for the HA, TB, and AL regions were 185.51μm^2/cm^3, 312.92 μm^2/cm^3, and 1075.37 μm^2/cm^3, respectively.

The percent of metal fume particles deposited on the three regions, while presented in sequence, were: (1) number: HA (18%), TB (24%), AL (58%); (2) mass: HA (11%), TB (18%), AL (71%); (3) surface area: HA (12%), TB (20%), AL (68%).

All the fractions of the metal fume particles deposited on the alveolar region were higher than the other two regions of the head airway, tracheobronchial.

According to the above results, we could use the estimated regional particle depositions to provide different respiratory protective equipment for the LMD workers.

Table 6 Regional particle depositions (values in parentheses) of metal fume particles deposited on the HA, TB, and AL regions for the LMD chamber

	Head airways (HA)	Tracheobronchial (TB)	Alveolar (AL)	Total
Number concentrations (#/cm^3)	1.73×10^5 (18%)	2.38×10^5 (24%)	5.72×10^5 (58%)	9.83×10^5 (100%)
Mass concentrations (μg/cm^3)	8.77×10^{-8} (11%)	1.54×10^{-7} (18%)	5.91×10^{-7} (71%)	8.33×10^{-7} (100%)
Surface area concentrations (μm^2/cm^3)	185.51 (12%)	312.92 (20%)	1075.37 (68%)	1573.80 (100%)

(3). Heavy metal concentrations of metal fume particles from the LMD process

The concentrations of nickel and chromium were analyzed by ICP-MS are shown in Figs. 11(a) and (b). The figures showed the error bars on the plots are large, the possible explanation for this may lie in the powder feeder is not stable. The mass concentration compositions of the metal powder in this study is the same as Zhang et al. (2011), and Zhang et al. (2011) found the mass percent of the LMD layer of nickel and chromium were about 53% and 20%, respectively, the results showed that the ratio of nickel and chromium is roughly consistent with the SDS (Zhang et al. 2011), that is, all the nickel and the chromium in the metal powder are melted due to high-temperature heating, and for a pressure of 100kPa, the temperature of nickel and chromium will be approximately 3184K and 2942K, respectively, the temperature of nickel is nearly the same as chromium at same vapor pressure, this may result in the heavy metal concentrations of chromium were almost the same as the nickel. And according to Sreekanthan (1997), the hexavalent chromium was present in amounts ranging from 0.29 to 2.05 percent by weight of the chrome content in fume (Sreekanthan 1997). Therefore, we adopted 2.05 percent by weight of total chromium as the concentration of hexavalent chromium to assess the exposure for the LMD workers.

The average heavy metal concentrations of nickel, chromium (III) and (VI) were 83.62 ± 36.19 μg/m^3, 85.51 ± 17.60 μg/m^3, and 1.79 ± 0.37 μg/m^3, respectively, and the values of 95%-tile were 161.07μg/m^3, 115.35 μg/m^3, and 2.41 μg/m^3, respectively.

The 95%-tile concentration of nickel exceeded the STEL (Short-term exposure limit) proposed in Russia (50 μg/m³) and Hungary (5μg/m³), but the 95%-tile concentrations of chromium (III) and (VI) didn't exceed the STEL proposed in Taiwan (0.15 μg/m³ and 0.015μg/m³).

At no time shall the LMD operation be used where workers exposure levels for the metal fumes exceed the established standards for those components. According to the AIHA exposure control strategy, exposures exceeded the standards require adequate respirators, engineering controls, and work practice controls provided (AIHA 2015). Hence, the LMD chamber was offered an enclosure ventilation system to reduce the emission of metal fume particles.
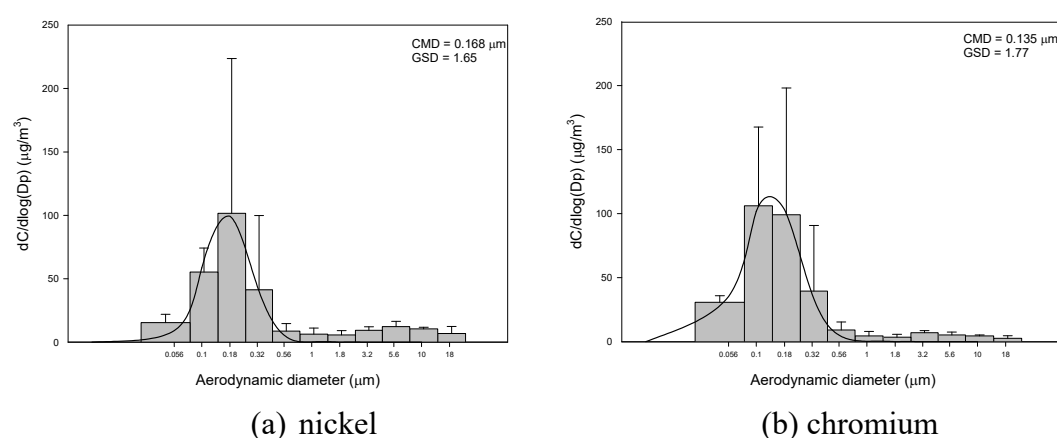

(a) nickel   (b) chromium

Figure 11 The heavy metal concentration measured by ICP-MS

(4). Health risk assessments of metal fume particles from the LMD process

For both the heavy metal content concentrations of the Ni and the Cr(VI), cancer risk (CR) estimates were evaluated relative to the standard USEPA acceptable risk range of 1×10^{-6} (USEPA 1990).

The sampled filters in MOUDI, which analyzed nickel and chromium, total cancer risk estimates was without the acceptable cancer risk range: 1.16×10^{-4} or the 95%-tile: 1.62×10^{-4}, was outside of the acceptable cancer risk range of 1.0×10^{-6}, the resultant cancer risk is unacceptable. That is if the workers enter the LMD chamber without engineering control might encounter potential health hazards, so it's important to take actions to protect the workers from hazards.

(5). Air velocity gradient in the LMD chamber

In this study, the LMD chamber airflow velocity was measured using an air velocity meter. Twelve measurement points in an equally spaced 3 by 4 grid were located within the chamber at length of 0.45, 1.35, 2.25, and 3.15 m, the airflow velocity gradient diagrams as shown in Figs. 12 , and the ACH of the chamber is 100. The ability of the source enclosure ventilation system to reduce exposure to air contaminants is determined by the capture velocities of the hoods, we found the

capture velocities of the hoods were greater than the standards values proposed by HSE. Therefore, the air flow could be effectively used to contain and capture the metal fume particles in the LMD chamber.
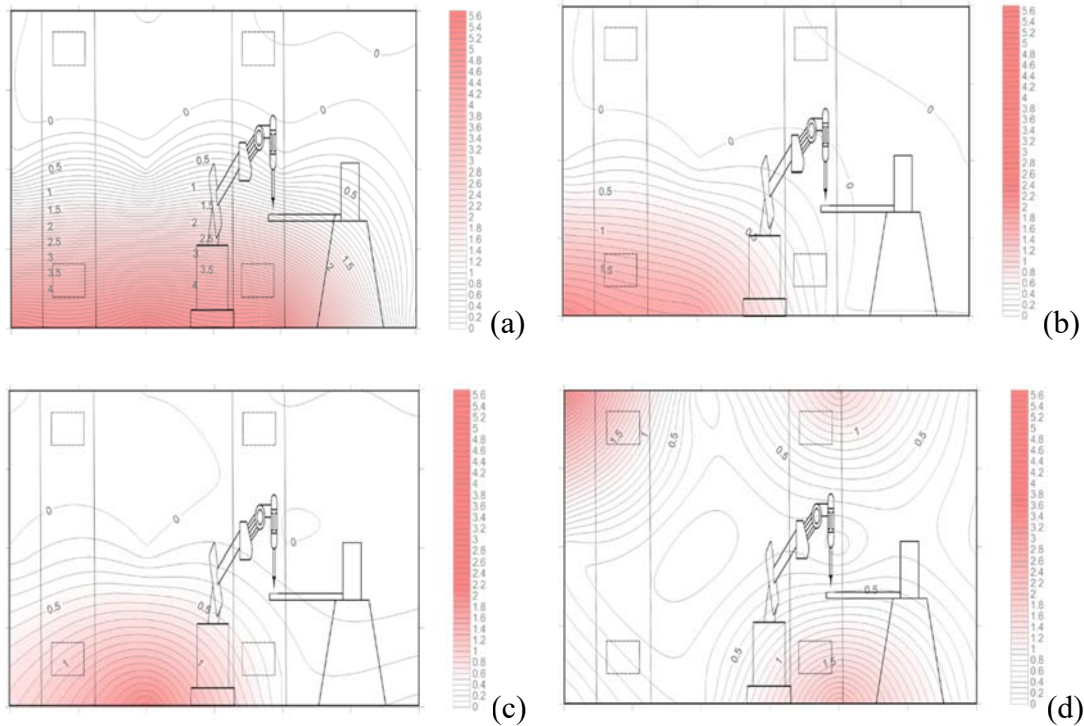

Figure 12 The air velocity gradient diagram at the length of (a) 0.45 m, (b) 1.35 m, (c) 2.25 m, (d) 3.15 m.

(6). Emission rate and emission factor

From the particle number concentrations obtained through the SMPS, emission rate (ER) and emission factor (EF) were calculated. The values of ER and EF were found as 1.2×10^{10} #/min and 4.67×10^{8} #/g, respectively. In our experimental results obviously indicate that the high emission factors during the LMD processes. In order to reduce the health effects of metal fumes, it is suggested that the installations of a ventilation system coupled with a local exhaust ventilation are necessary in order to reduce exposures to the workers.

As to the emission rates derived from this study can be compared with those presented in the literature, for example, the welding or 3D printing activities, however, there is no literature which is related to the laser metal deposition process or the activity as the same as in this study, so the ERs and the EFs in this study can be used as a reference for future research.

(7). Particle concentrations generated by different LMD time

    A.   Particle size distributions for different LMD time

For particle number concentrations, it can be seen that the particle number distributions of each LMD time were uni-modal, and there is no significant difference

in the CMDs and GSDs for each LMD time, the ranges of the CMD and GSD are 0.020 – 0.021 μm and 1.87 – 1.96, respectively. Similar trends of size distributions were also found in mass and surface area concentration, the MMD was 0.0465 ± 0.0015 μm with GSD of 1.83 ± 0.03, respectively; the SMD was 0.037 ± 0.001 μm with GSD of 1.845 ± 0.035, respectively. A result summary is listed in Table 7.

Table 7 Particle size distributions for different LMD time

LMD time	1 min	2 min	3 min	4 min	5 min
CMD (μm)	0.020	0.020	0.021	0.021	0.021
Total number conc. (#/cm^3)	7.77×10^{11}	8.37×10^{11}	8.42×10^{11}	8.48×10^{11}	8.55×10^{11}
MMD (μm)	0.045	0.045	0.046	0.047	0.048
Total mass conc. (μg/m^3)	2.13×10^9	2.28×10^9	2.28×10^9	2.28×10^9	2.29×10^9
SMD (μm)	0.036	0.037	0.037	0.037	0.038
Total surface area conc. (μm^2/cm^3)	4.60×10^7	8.16×10^7	1.002×10^8	1.80×10^8	1.37×10^8

B. Predicted regional particle depositions for different LMD time

In this study, the resultant size distribution data was further used to estimate particle concentrations of metal fume particles deposited on different regions of the respiratory tract for each LMD time. Table 8 shows the estimated particle concentrations (and their percents) deposited on the three regions of the HA, TB, and AL of the respiratory tract. Similar trends were found for the percent of metal fume particles deposited on the three regions, as AL > TB > HA, the results clearly indicate that the fractions of metal fume particles deposited on the AL region were much higher than that of the other two regions.

Thus, if the workers need to enter the LMD chamber without taking engineering control, it can expose workers to inhale metal fume particles, it's necessary to use the respirator for workers, and according to the results, higher forms of respiratory protection must be used since respirators with an assigned protection factor (APF) of 10 are not sufficient for high particle concentration exposures.

Table 8 Regional particle depositions (values in parentheses) of metal fume particles deposited on the HA, TB, and AL regions for each LMD time

LMD time	Type	Head airways (HA)	Tracheobronchial (TB)	Alveolar (AL)	Total
1 min	Number	2.43×10^9 (16%)	3.49×10^9	8.81×10^9	1.47×10^{10}

	concentrations (#/cm³)		(24%)	(60%)	(100%)
	Mass concentrations (µg/cm³)	2.75×10^{-3} (11%)	4.73×10^{-3} (20%)	1.68×10^{-2} (69%)	2.42×10^{-2} (100%)
	Surface area concentrations (µm²/cm³)	1.12×10^{7} (12%)	1.85×10^{7} (21%)	5.97×10^{7} (67%)	8.94×10^{7} (100%)
2 min	Number concentrations (#/cm³)	4.33×10^{9} (16%)	6.16×10^{9} (24%)	1.55×10^{10} (60%)	2.60×10^{10} (100%)
	Mass concentrations (µg/cm³)	4.85×10^{-3} (11%)	8.34×10^{-3} (20%)	2.96×10^{-2} (69%)	4.28×10^{-2} (100%)
	Surface area concentrations (µm²/cm³)	2.03×10^{7} (12%)	3.33×10^{7} (21%)	1.08×10^{8} (67%)	1.61×10^{8} (100%)
3 min	Number concentrations (#/cm³)	5.38×10^{9} (17%)	7.59×10^{9} (24%)	1.88×10^{10} (59%)	3.18×10^{10} (100%)
	Mass concentrations (µg/cm³)	5.92×10^{-3} (11%)	1.02×10^{-3} (20%)	3.62×10^{-2} (69%)	5.23×10^{-2} (100%)
	Surface area concentrations (µm²/cm³)	2.57×10^{7} (12%)	4.20×10^{7} (21%)	1.36×10^{8} (67%)	2.03×10^{8} (100%)
4 min	Number concentrations (#/cm³)	5.94×10^{9} (17%)	8.30×10^{9} (24%)	2.03×10^{10} (59%)	3.46×10^{10} (100%)
	Mass concentrations (µg/cm³)	6.37×10^{-3} (11%)	1.10×10^{-2} (20%)	3.90×10^{-2} (69%)	5.63×10^{-2} (100%)
	Surface area concentrations (µm²/cm³)	2.86×10^{7} (12%)	4.67×10^{7} (21%)	1.50×10^{8} (67%)	2.26×10^{8} (100%)
5 min	Number concentrations (#/cm³)	7.98×10^{9} (18%)	1.09×10^{10} (24%)	2.59×10^{10} (58%)	4.47×10^{10} (100%)
	Mass concentrations (µg/cm³)	8.01×10^{-3} (11%)	1.38×10^{-3} (20%)	4.89×10^{-2} (69%)	7.07×10^{-2} (100%)
	Surface area concentrations (µm²/cm³)	3.89×10^{7} (13%)	6.32×10^{7} (21%)	2.02×10^{8} (66%)	3.04×10^{8} (100%)

(8). Suitable ventilation time at different LMD time

After LMD operation, it is important how fast the metal fume particles are removed by using ventilation system to protect workers. The times it takes for the

particle concentrations to reduce down to background levels or the cancer risk to be within the acceptable value (10^{-6}) for different LMD time is shown in Table 9 and Figs. 13 , for different LMD time, it took different ventilation times to reach the background levels or acceptable range in the chamber for different metrics, in approximately 13 minutes for number concentrations; in 10 minutes for particle mass concentrations; in 10 minutes for surface area concentrations, and in 7 minutes for cancer risk to reach the acceptable value, respectively, due to lacking the data that the heavy metal concentrations sampled by MOUDI for 1-4 minutes, we couldn't obtain the values of ventilation time for 1-4 minutes, but the ventilation time of the cancer risk for each LMD time (1-4 minutes) should be less than 6.03 minutes theoretically.

Because there is no exposure limit value for the metal fume particles emitted from the LMD process, we assessed different exposure metrics of the metal fume particles to determine the ventilation times, the results showed most the longest ventilation time were contributed from the particle number concentrations, thus the recommendation for exposure metric is the particle number concentrations, the required ventilation time for each LMD time would use the data which were obtained from particle number concentrations.
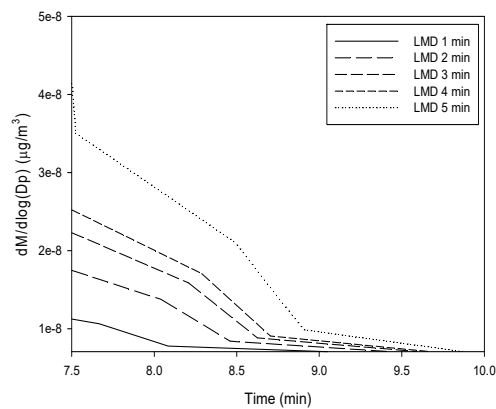
Table 9 The ventilation time for different particle concentration to each LMD time

LMD time	Required ventilation time (min)				
	1 min	2 min	3 min	4 min	5 min
Number conc.	11.91	12.23	12.32	12.34	12.43
Mass conc.	9.05	9.43	9.59	9.67	9.87
Surface area conc.	8.83	9.21	9.37	9.45	9.65
Cancer risk	<6.03*	<6.03*	<6.03*	<6.03*	6.03

*unavailable, theoretically less than 6.03 minutes.
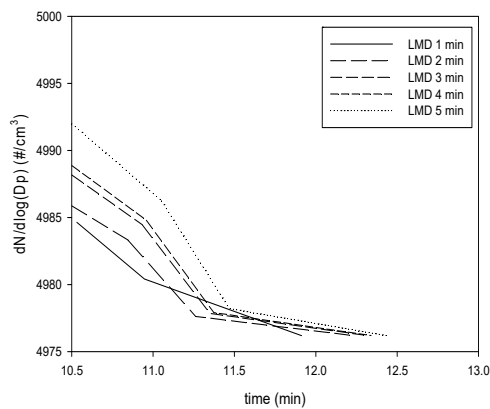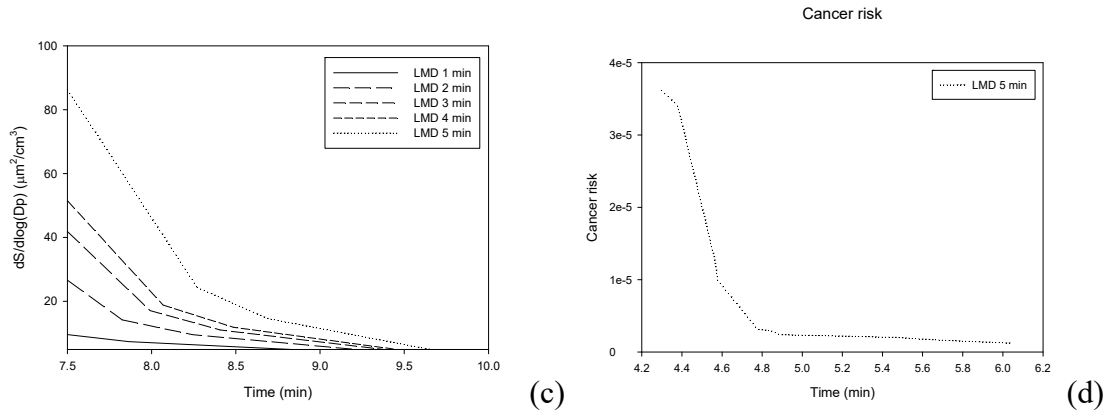

(a)   (b)

Figure 13 The ventilation time for different metrics to each LMD time, (a) number concentration, (b) mass concentration, (c) surface area concentration, (d) cancer risk.

Conclusions and recommendations

Particles emitted from the LMD process were in the form of the bimodal show that the metal fumes contain nanoparticles and the fraction of particles deposited on the AL region was higher than that of the other two regions. The emitted heavy metal concentrations and the resultant health risks were found to be unacceptable. The present study suggests a ventilation time of 13 minutes for the LMD process for a general exhaust system with 100 ACH. It is recommended to use the computational fluid dynamics (CFD) software to estimate the particle concentrations for different LMD time, so that we can analyze different operating conditions to establish a model for the LMD process from the data and the fluid flow which are computed.

Reference

AIHA AIHA. 2015. A strategy for assessing and managing occupational exposure. USA.

Antonini JM, Lewis AB, Roberts JR, Whaley DA. 2003. Pulmonary effects of welding fumes: Review of worker and experimental animal studies. American journal of industrial medicine 43:350-360.

Azimi P, Zhao D, Pouzet C, Crain NE, Stephens B. 2016. Emissions of ultrafine particles and volatile organic compounds from commercially available desktop three-dimensional printers with multiple filaments. Environmental science & technology 50:1260-1268.

Barcikowski S, Hahn A, Kabashin A, Chichkov B. 2007. Properties of nanoparticles generated during femtosecond laser machining in air and water. Applied Physics A 87:47-55.

Buonanno G, Morawska L, Stabile L. 2009. Particle emission factors during cooking activities. Atmospheric Environment 43:3235-3242.

Buonanno G, Morawska L, Stabile L. 2011. Exposure to welding particles in automotive plants. Journal of Aerosol Science 42:295-304.

Buzea C, Pacheco II, Robbie K. 2007. Nanomaterials and nanoparticles: Sources and toxicity. Biointerphases 2:MR17-MR71.

Chao CY, Wan M, Cheng EC. 2003. Penetration coefficient and deposition rate as a function of particle size in non-smoking naturally ventilated residences. Atmospheric Environment 37:4233-4241.

Chiung Y-mH, Chun-ming; Liu,Pei-shan. 2011. Cell toxicity and worker health caused by nano-sized metals from laser-cutting process. Institute of Labor, Occupational Safety And Health, Ministry of Labor IOSH99-M324.

Demou E, Peter P, Hellweg S. 2008. Exposure to manufactured nanostructured particles in an industrial pilot plant. Annals of Occupational Hygiene 52:695-706.

Demou E, Stark WJ, Hellweg S. 2009. Particle emission and exposure during nanoparticle synthesis in research laboratories. Annals of occupational hygiene 53:829-838.

Donaldson K, Li X, MacNee W. 1998. Ultrafine (nanometre) particle mediated lung injury. Journal of Aerosol Science 29:553-560.

Donaldson K, Tran L, Jimenez LA, Duffin R, Newby DE, Mills N, et al. 2005. Combustion-derived nanoparticles: A review of their toxicology following inhalation exposure. Particle and fibre toxicology 2:10.

Elihn K, Berg P. 2009. Ultrafine particle characteristics in seven industrial plants. Annals of Occupational Hygiene:mep033.

Elsaesser A, Howard CV. 2012. Toxicology of nanoparticles. Advanced drug delivery reviews 64:129-137.

Ferreira-Baptista L, De Miguel E. 2005. Geochemistry and risk assessment of street dust in luanda, angola: A tropical urban environment. Atmospheric Environment 39:4501-4512.

Fuks NA. 1989. The mechanics of aerosols:Dover Publications.

Gatoo MA, Naseem S, Arfat MY, Mahmood Dar A, Qasim K, Zubair S. 2014. Physicochemical properties of nanomaterials: Implication in associated toxic manifestations. BioMed research international 2014.

Gonser M, Hogan T. 2011. Arc welding health effects, fume formation mechanisms, and characterization methods. In: Arc welding:InTech.

Gray C, Hewitt P, Dare P. 1983. New approach would help control weld fumes at source. Part three: Mma fumes.

Grinshpun S, Lipatov G, Sutugin A. 1990. Sampling errors in cylindrical nozzles. Aerosol Science and Technology 12:716-740.

Grinshpun S, Willeke K, Kalatoor S. 1993. A general equation for aerosol aspiration

by thin-walled sampling probes in calm and moving air. Atmospheric Environment Part A General Topics 27:1459-1470.

Gu D, Meiners W, Wissenbach K, Poprawe R. 2012. Laser additive manufacturing of metallic components: Materials, processes and mechanisms. International materials reviews 57:133-164.

Han JH, Lee EJ, Lee JH, So KP, Lee YH, Bae GN, et al. 2008. Monitoring multiwalled carbon nanotube exposure in carbon nanotube research facility. Inhalation toxicology 20:741-749.

Hinds WC. 2012. Aerosol technology: Properties, behavior, and measurement of airborne particles:John Wiley & Sons.

Howard-Reed C, Wallace LA, Emmerich SJ. 2003. Effect of ventilation systems and air filters on decay rates of particles produced by indoor sources in an occupied townhouse. Atmospheric Environment 37:5295-5306.

HSE HaSE. 2014. Local exhaust ventilation (lev) guidance. HSE.

ICRP ICoRP. 1994. Human respiratory tract model for radiological protection, publication 66,annals of icrp.

Khlystov A, Stanier C, Pandis S. 2004. An algorithm for combining electrical mobility and aerodynamic size distributions data when measuring ambient aerosol special issue of aerosol science and technology on findings from the fine particulate matter supersites program. Aerosol Science and Technology 38:229-238.

Kim Y, Yoon C, Ham S, Park J, Kim S, Kwon O, et al. 2015. Emissions of nanoparticles and gaseous material from 3d printer operation. Environmental Science & Technology 49:12044-12053.

Kyogoku H. 2014. < レビュー> 金属 3d プリンタの開発動向と今後の展開. 近畿大学次世代基盤技術研究所報告 5:139-143.

Lee M-H, McClellan WJ, Candela J, Andrews D, Biswas P. 2006. Reduction of nanoparticle exposure to welding aerosols by modification of the ventilation system in a workplace. In: Nanotechnology and occupational health:Springer, 127-136.

Marple VA, Rubow KL, Behm SM. 1991. A microorifice uniform deposit impactor (moudi): Description, calibration, and use. Aerosol Science and Technology 14:434-446.

Maynard AD. 2003. Estimating aerosol surface area from number and mass concentration measurements. Annals of Occupational Hygiene 47:123-144.

Maynard AD, Kuempel ED. 2005. Airborne nanostructured particles and occupational health. Journal of nanoparticle research 7:587-614.

McCann B, Hunter R, McCann J. 2002. Cocaine/heroin induced rhabdomyolysis and ventricular fibrillation. Emergency Medicine Journal 19:264-264.

Meeker JD, Susi P, Flynn MR. 2007. Manganese and welding fume exposure and

control in construction. Journal of occupational and environmental hygiene 4:943-951.

Mueller EJ, Seger DL. 1985. Metal fume fever—a review. The Journal of emergency medicine 2:271-274.

Nemery B. 1990. Metal toxicity and the respiratory tract. European Respiratory Journal 3:202-219.

Nielsen E, Dybdahl M, Larsen PB, Miljøstyrelsen D, Risikovurdering FAfTo. 2008. Health effects assessment of exposure to particles from wood smoke:Danish Environmental Protection Agency.

NIOSH NIfOSaH. 2014. Current strategies for engineering controls in nanomaterial production and downstream handling processes Department of health and human services 2014-102.

NIOSH TNIfOSaH. 2016. Hierarchy of controls. Workplace Safety & Health Topics.

Oberdörster G, Oberdörster E, Oberdörster J. 2005. Nanotoxicology: An emerging discipline evolving from studies of ultrafine particles. Environmental health perspectives:823-839.

OSHA OSaHA. 2009. Assigned protection factors for the revised respiratory protection standard. OSHA OSHA 3352-02.

Pagels J, Wierzbicka A, Nilsson E, Isaxon C, Dahl A, Gudmundsson A, et al. 2009. Chemical composition and mass emission factors of candle smoke particles. Journal of Aerosol Science 40:193-208.

Palmer KT, Poole J, Ayres JG, Mann J, Burge PS, Coggon D. 2003. Exposure to metal fume and infectious pneumonia. American Journal of Epidemiology 157:227-233.

Park K, Cao F, Kittelson DB, McMurry PH. 2003. Relationship between particle mass and mobility for diesel exhaust particles. Environmental Science & Technology 37:577-583.

Peters TM, Leith D. 2003. Concentration measurement and counting efficiency of the aerodynamic particle sizer 3321. Journal of Aerosol Science 34:627-634.

Schulte P, Geraci C, Zumwalde R, Hoover M, Kuempel E. 2008. Occupational risk management of engineered nanoparticles. Journal of occupational and environmental hygiene 5:239-249.

Sreekanthan P. 1997. Study of chromium in welding fume.

Stabile L, Fuoco F, Buonanno G. 2012. Characteristics of particles and black carbon emitted by combustion of incenses, candles and anti-mosquito products. Building and Environment 56:184-191.

Stephens B, Azimi P, El Orch Z, Ramos T. 2013. Ultrafine particle emissions from desktop 3d printers. Atmospheric Environment 79:334-339.

Tsai S-JC, Huang RF, Ellenbecker MJ. 2010. Airborne nanoparticle exposures while

using constant-flow, constant-velocity, and air-curtain-isolated fume hoods. Annals of occupational hygiene 54:78-87.

USEPA USEPA. 1990. National oil and hazardous substances pollution contingency plan; final rule. 40 CFR part 300.

USEPA USEPA. 2009. Risk assessment guidance for superfund, volume i: Human health evaluation manual (part f, supplemental guidance for inhalation risk assessment), final. Environmental Protection Agency EPA-540-R-070-002, OSWER 9285.7-82.

USEPA USEPA. 2014. Chapter three of the sw-846 compendium: Inorganic analytes. Environmental Protection Agency SW846 Revision 5.

Wehner B, Uhrner U, Von Löwis S, Zallinger M, Wiedensohler A. 2009. Aerosol number size distributions within the exhaust plume of a diesel and a gasoline passenger car under on-road conditions and determination of emission factors. Atmospheric Environment 43:1235-1245.

Xu M, Nematollahi M, Sextro RG, Gadgil AJ, Nazaroff WW. 1994. Deposition of tobacco smoke particles in a low ventilation room. Aerosol Science and Technology 20:194-206.

Zai S, Zhen H, Jia-song W. 2006. Studies on the size distribution, number and mass emission factors of candle particles characterized by modes of burning. Journal of aerosol science 37:1484-1496.

Zhang Q-l, Yao J-h, Mazumder J. 2011. Laser direct metal deposition technology and microstructure and composition segregation of inconel 718 superalloy. Journal of Iron and Steel Research, International 18:73-78.

Zhong C, Chen J, Linnenbrink S, Gasser A, Sui S, Poprawe R. 2016a. A comparative study of inconel 718 formed by high deposition rate laser metal deposition with ga powder and prep powder. Materials & Design.

Zhong C, Gasser A, Kittel J, Wissenbach K, Poprawe R. 2016b. Improvement of material performance of inconel 718 formed by high deposition-rate laser metal deposition. Materials & Design 98:128-134.

科技部補助專題研究計畫出席國際學術會議心得報告

計畫編號	MOST 106-2221-E-040-001
計畫名稱	雷射金屬沉積作業人員奈米暴露評估控制指標之開發與應用
出國人員姓名	王櫻芳
服務機構及職稱	中山醫學大學 職業安全衛生學系 助理教授
會議時間	107 年 06 月 17 日至 107 年 06 月 20 日
會議地點	西班牙,畢爾包
會議名稱	(中文)2018 氣膠技術年會 (英文)Aerosol Technology 2018 (AT 2018)
發表題目	(中文) 雷射金屬沉積作業奈米暴露評估與控制策略 (英文) Assessing nanoparticle exposures associated with the laser metal deposition (LMD) operating process and its control strategy

一、參加會議經過

報告人與同行另一名報告者郭昱杰博士(成功大學環境醫學研究所)一起於 6 月 18 日參與會議開幕式，並選擇 Aerosols and Health 此 session 聆聽其他學者之相關研究之發表。於 6 月 19 日發表論文與參加 poster 之展示，並參觀現場展覽廠商有關最新以商業化之氣膠量測儀器。6 月 20 日則選擇 Indoor and Workplace environments 與 Aerosol sampling 此兩 session 聆聽其他學者之發表。
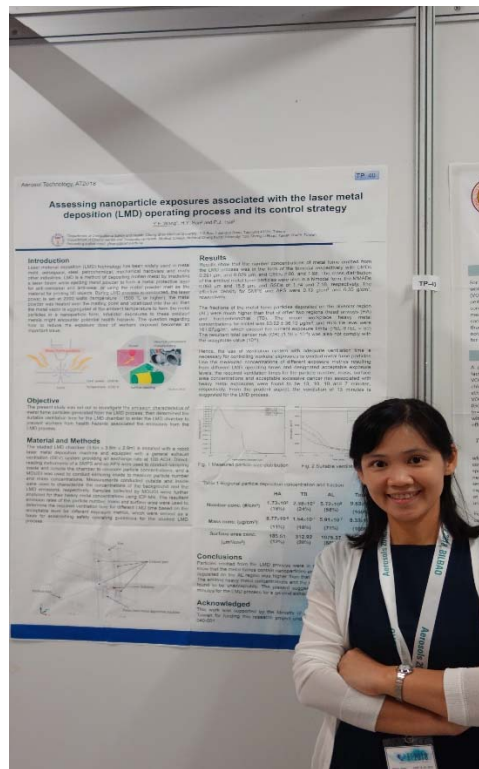
二、與會心得

本人之研究主軸在於奈米氣膠、氣膠之暴露評估技術與健康危害，故參加期間主要以 Aerosols and Health, Nanoparticles, Aerosol sampling, Indoor and workplace environments 等 sessions 之演講為主，並於每天下午 16：00~18：30 參加 poster 之展示，及與各國研究者討論。

本次研究會發現目前 Aerosol 相關之研究仍以大氣氣膠量測之研究佔最大宗，因其涉及區域性差異，量測技術之更新，及大眾之普遍關注。值得注意的其所需求之設備價格昂貴，對國內研究者無法負荷，對長期競爭力將勢必

有所影響。奈米議題之研究在量測技術方面已日趨成熟，唯有關其奈米毒性方面之研究，仍有相當大的空間，特別是在與其他危害因子(含物理、化學及心理性因子)共存時之危害更值得探討。

三、發表論文全文或摘要

1. Introduction

Laser material deposition (LMD) technology has been widely used in metal mold, aerospace, steel, petrochemical, mechanical hardware and many other industries. LMD is a method of depositing molten metal by irradiating a laser beam while ejecting metal powder to form a metal protective layer for anti-corrosion and anti-wear, or using the metal powder melt as the material for printing 3D objects. During LMD process is conducted, the laser power is set at 2000 watts (temperature : 1500 ℃ or higher), the metal powder was heated over the melting point and volatilized into the air, then the metal vapor is aggregated at the ambient temperature to form the metal particles in a nanoparticle form. Inhalator exposures to these oxidized metals might encounter potential health hazards. The question regarding how to reduce the exposure dose of workers exposed becomes an important issue.

2. Objective

The present study was set out to investigate the emission characteristics of metal fume particles generated from the LMD process, then determined the suitable ventilation time for the LMD chamber to enter the LMD chamber to prevent workers from health hazards associated the emissions from the LMD process.

3. Material and Methods

Figure 1 shows that the studied LMD chamber (3.6m × 3.8m × 2.9m) is

installed with a robot laser metal deposition machine and equipped with a general exhaust ventilation (GEV) system providing air exchange rate at 100 ACH. Direct-reading instruments of a SMPS and an APS were used to conduct sampling inside and outside the chamber to measure particle concentrations, and a MOUDI was used to conduct sampling inside to measure particle number and mass concentrations. Measurements conducted outside and inside were used to characterize the concentrations of the background and the LMD emissions, respectively. Samples collected by MOUDI were further analyzed for their heavy metal concentrations using ICP-MS. The resultant emission rates of the particle number, mass and surface area were used to determine the required ventilation time for different LMD time based on the acceptable level for different exposure metrics, which were served as a basis for establishing safety operating guidelines for the studied LMD process.
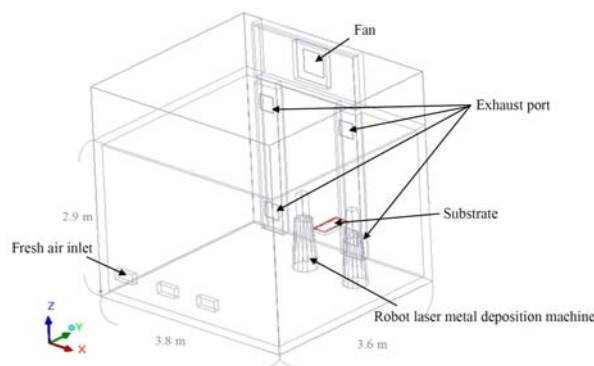

Figure 1 LMD chamber

4. Results

Figure 2 shows that the number concentrations of metal fume emitted from the LMD process was in the form of the bimodal respectively with CMDs 0.291 μm, and 0.029 μm, and GSDs 2.80, and 1.88. The mass distribution of the emitted metal fume particles were also in a bimodal form, the MMADs 0.068 μm and 15.5 μm, and GSDs of 1.74 and 7.18, respectively. The effective density for

SMPS and APS were 0.13 g/cm^3 and 0.35 g/cm^3, respectively.

The fractions of the metal fume particles deposited on the alveolar region (AL) were much higher than that of other two regions (head airways (HA) and tracheobronchial (TB). The mean workplace heavy metal concentrations for nickel was 83.62 ± 36.19 μg/m^3, and 95%-tile level were 161.07μg/m^3, which exceed the current exposure limits (PEL-STEL = 50) The resultant total cancer risk (CR) (1.16 × 10^{-4}) was also not comply with the acceptable value (10^{-6}).

Hence, the use of ventilation system with adequate ventilation time is necessary for controlling workers' exposures to emitted metal fume particles. Use the measured concentrations of different exposure metrics resulting from different LMD operating times and designated acceptable exposure levels, the required ventilation times for the particle number, mass, surface area concentrations and acceptable excessive cancer risk associated with heavy metal exposures were found to be 13, 10, 10 and 7 minutes, respectively (Figure 3). From the prudent aspect, the ventilation of 13 minutes is suggested for the LMD process.
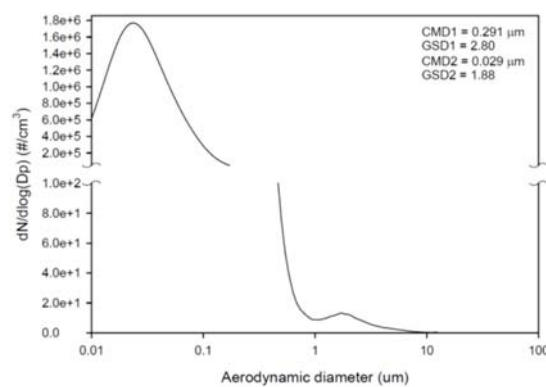

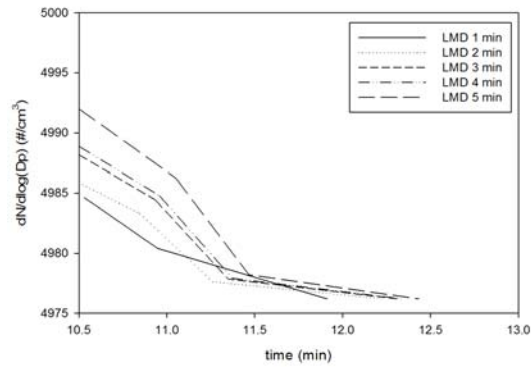Figure 2 Measured particle size distribution

Figure 3 Suitable ventilation time

5. Conclusions

Particles emitted from the LMD process were in the form of the bimodal show that the metal fumes contain nanoparticles and the fraction of particles deposited on the AL region was higher than that of the other two regions. The emitted heavy metal concentrations and the resultant health risks were found to be unacceptable. The present suggest a ventilation time of 13 minutes for the LMD process for a general exhaust system with 100 ACH.

三、建議

希望科技部多補助類似此區域性的重要會議,因為此種會議參與人數不像世界性會議那麼多,比較有機會能夠個別接觸重要的研究者。也希望能多讓研究生們出國開會,增廣見聞,提升視野,並激發研究生們(特別是碩士班學生)繼續深造的企圖心。

四、攜回資料名稱及內容

AT 2018 Handbook 及論文摘要隨身碟一份

五、其他:無

106年度專題研究計畫成果彙整表

成果項目				量化	單位	質化 （說明：各成果項目請附佐證資料或細項說明，如期刊名稱、年份、卷期、起訖頁數、證號...等）
國內	學術性論文	期刊論文		0		
		研討會論文		1	篇	孫新怡、王櫻芳、蔡朋枝. 雷射金屬沉積製程中產生之金屬燻煙微粒特徵. 2017 職業衛生研討會, 台北, 台灣, Mar. 10-11, 2017.
		專書		0	本	
		專書論文		0	章	
		技術報告		0	篇	
		其他		0	篇	
	智慧財產權及成果	專利權	發明專利 申請中	0	件	
			發明專利 已獲得	0		
			新型/設計專利	0		
		商標權		0		
		營業秘密		0		
		積體電路電路布局權		0		
		著作權		0		
		品種權		0		
		其他		0		
	技術移轉	件數		0	件	
		收入		0	千元	
國外	學術性論文	期刊論文		0		
		研討會論文		2	篇	1.Yu-Hsuan Liu; Ying-Fang Wang, Characteristics of the particle size distribution and exposure concentrations of nanoparticles generated from the laser metal deposition process. 19th World academy of sciene, engineering and technology conference, Tokyo, Japan, Nov 13-15, 2017. 2.Y.F. Wang, H.Y. Sun and P.J. Tsai, Assessing nanoparticle exposures associated with the laser metal deposition (LMD) operating process and its control strategy. Aerosol Technology 2018, Bilbao, Spain, June 17-20, 2018.

		專書		0	本	
		專書論文		0	章	
		技術報告		0	篇	
		其他		0	篇	
	智慧財產權及成果	專利權	發明專利	申請中	0	件	
				已獲得	0		
			新型/設計專利	0		
		商標權		0		
		營業秘密		0		
		積體電路電路布局權		0		
		著作權		0		
		品種權		0		
		其他		0		
	技術移轉	件數		0	件	
		收入		0	千元	
參與計畫人力	本國籍	大專生		0	人次	
		碩士生		2		席珮瑄 蘇世心
		博士生		0		
		博士後研究員		0		
		專任助理		0		
	非本國籍	大專生		0		
		碩士生		0		
		博士生		0		
		博士後研究員		0		
		專任助理		0		
其他成果（無法以量化表達之成果如辦理學術活動、獲得獎項、重要國際合作、研究成果國際影響力及其他協助產業技術發展之具體效益事項等，請以文字敘述填列。）						

科技部補助專題研究計畫成果自評表

請就研究內容與原計畫相符程度、達成預期目標情況、研究成果之學術或應用價值（簡要敘述成果所代表之意義、價值、影響或進一步發展之可能性）、是否適合在學術期刊發表或申請專利、主要發現（簡要敘述成果是否具有政策應用參考價值及具影響公共利益之重大發現）或其他有關價值等，作一綜合評估。

---

1. 請就研究內容與原計畫相符程度、達成預期目標情況作一綜合評估
   ■達成目標
   □未達成目標（請說明，以100字為限）
   　　　□實驗失敗
   　　　□因故實驗中斷
   　　　□其他原因
   說明：

---

2. 研究成果在學術期刊發表或申請專利等情形（請於其他欄註明專利及技轉之證號、合約、申請及洽談等詳細資訊）
   論文：□已發表　■未發表之文稿　□撰寫中　□無
   專利：□已獲得　□申請中　■無
   技轉：□已技轉　□洽談中　■無
   其他：（以200字為限）

---

3. 請依學術成就、技術創新、社會影響等方面，評估研究成果之學術或應用價值（簡要敘述成果所代表之意義、價值、影響或進一步發展之可能性，以500字為限）
   此研究之結果，可協助類似作業場所採取適當防範對策及管理制度，可有效防止職業暴露之健康危害發生。

---

4. 主要發現
   本研究具有政策應用參考價值：■否　□是，建議提供機關
   （勾選「是」者，請列舉建議可提供施政參考之業務主管機關）
   本研究具影響公共利益之重大發現：□否　□是
   說明：（以150字為限）